Geochemistry Geophysics Geosystems G3
AN ELECTRONIC JOURNAL OF THE EARTH SCIENCES
Published by AGU and the Geochemical Society

*Article*
Volume 6, Number 11
29 November 2005
Q11H20, doi:10.1029/2005GC001001
ISSN: 1525-2027

# A geomagnetic paleointensity stack between 0.8 and 3.0 Ma from equatorial Pacific sediment cores

**Toshitsugu Yamazaki and Hirokuni Oda**

*Institute of Geology and Geoinformation, Geological Survey of Japan, AIST, 1-1-1 Higashi, Tsukuba 305-8567, Japan (toshi-yamazaki@aist.go.jp)*

[1] We have conducted a paleomagnetic study of six sediment cores taken from the equatorial Pacific, three from the West Caroline Basin and three from the Manihiki Plateau, in order to make a relative paleointensity stack during the Matuyama and late Gauss Chrons. The age of the bottom of the cores ranges from 1.2 to 3.0 Ma. The sediments show little downcore changes in the proxies of magnetic grain size and mineralogy and are hence suitable for estimating relative paleointensity. The age of the cores is controlled by correlating variations in magnetic concentration (magnetic susceptibility and/or anhysteretic remanent magnetization (ARM)) to target oxygen-isotope ($\delta^{18}O$) curves. All cores from the Manihiki Plateau show an upward decrease of the natural remanent magnetization (NRM) intensity normalized by ARM and isothermal remanent magnetization (IRM) with a decrease in sedimentation rate. Such a trend was removed before being converted to relative paleointensity. This observation implies that a sedimentation-rate change can affect relative paleointensity estimation. Relative paleointensity records from the six cores coincide well with each other within uncertainty of age. We constructed a stacked curve between 0.8 and 3.0 Ma (the equatorial Pacific paleointensity stack EPAPIS-3Ma) after adjusting age; the number of cores stacked is three to four throughout the record. Quasiperiodic paleointensity lows occur in the EPAPIS-3Ma, and corresponding paleointensity lows can be found in previously published records with some shifts in age. At least, parts of the paleointensity minima seem to be accompanied by geomagnetic excursions. The "asymmetric sawtooth pattern" of paleointensity variations is not observed at the Matuyama-Gauss boundary and thereafter in our record. A spectral analysis shows that ~100 kyr orbital eccentricity frequency may exist in paleointensity variations during the Matuyama and late Gauss Chrons.

**Components:** 8401 words, 20 figures, 1 table.

**Keywords:** equatorial Pacific; excursion; orbital modulation; paleointensity; paleomagnetism.

**Index Terms:** 1513 Geomagnetism and Paleomagnetism: Geomagnetic excursions; 1521 Geomagnetism and Paleomagnetism: Paleointensity; 1594 Geomagnetism and Paleomagnetism: Instruments and techniques.

**Received** 17 April 2005; **Revised** 29 August 2005; **Accepted** 14 October 2005; **Published** 29 November 2005.

Yamazaki, T., and H. Oda (2005), A geomagnetic paleointensity stack between 0.8 and 3.0 Ma from equatorial Pacific sediment cores, *Geochem. Geophys. Geosyst.*, *6*, Q11H20, doi:10.1029/2005GC001001.

**Theme:** Geomagnetic Field Behavior Over the Past 5 Myr
**Guest Editors:** Cathy Constable and Catherine Johnson

## 1. Introduction

[2] In the 1990s, studies on recovering relative changes of the intensity of the past geomagnetic field (paleointensity) progressed significantly using marine sediment cores. Accumulation of relative paleointensity records during the Brunhes Chron resulted in establishment of the stacked paleointen-

sity curve during the last 800 kyr, the Sint-800 curve [*Guyodo and Valet*, 1999]. Since then, one way of relative paleointensity studies is toward obtaining higher-resolution records during the last ca. 100 kyr like the North Atlantic paleointensity stack NAPIS-75 [*Laj et al.*, 2000]. High resolution relative paleointensity curves are quite useful for high-resolution chronostratigraphy. Recent studies demonstrated a potential of paleointensity as a high-resolution global correlation tool in the late Pleistocene [e.g., *Stoner et al.*, 2000]. Another course of paleointensity studies is toward extending records back to ages older than the Brunhes Chron. Several relative paleointensity records extending to the Matuyama Chron have been reported so far [*Meynadier et al.*, 1994; *Kok and Tauxe*, 1999; *Channell et al.*, 2002, *Yamazaki and Oda*, 2002; *Carcaillet et al.*, 2003; *Horng et al.*, 2003], and a stacked record from the Ontong-Java Plateau (the OJP-stack [*Kok and Tauxe*, 1999]) reached 3 Ma. As pointed out by *Channell et al.* [2002], however, these records are not in good agreement with each other, partly because of poor age control.

[3] In 1993, *Valet and Meynadier* [1993] presented a paleointensity record since 4 Ma using cores of the Ocean Drilling Program (ODP) Leg 138, and postulated the "asymmetric sawtooth pattern" of paleointensity variations; the geomagnetic field rapidly grows immediately after polarity reversals, whereas it decays slowly during stable polarity periods, and the length of a polarity is proportional to the amount of an intensity jump at the beginning of the polarity period. If this is true, this implies that the state of the core just after a polarity reversal controls the geodynamo for a long period of time, which contradicts the general thought that the core cannot have a long-term memory. This hypothesis has raised heated arguments, in particular on the possibility that it is an artifact caused by remanent magnetization acquisition processes [e.g., *Kok and Tauxe*, 1996; *Mazaud*, 1996]. Reproducibility of the "sawtooth pattern" has not yet been fully tested even in the early Matuyama Chron. Except for the records used for proposing the "sawtooth pattern" [*Valet and Meynadier*, 1993; *Meynadier et al.*, 1994], the OJP-stack of *Kok and Tauxe* [1999] would be the only continuous paleointensity record which reached the Matuyama-Gauss (G/M) boundary, and this record did not support the "sawtooth pattern."

[4] Another recent argument from relative paleointensity data is a possibility of orbital modulation of the geomagnetic field. *Channell et al.* [1998] found ~41 kyr orbital obliquity frequency in their paleointensity records during the Brunhes Chron from ODP Sites 983 and 984. *Yamazaki* [1999] and *Yokoyama and Yamazaki* [2000] instead found ~100 kyr eccentricity frequency in the paleointensity records during the Brunhes Chron from Pacific sediment cores. *Horng et al.* [2003] argued that the orbital frequencies in paleointensity variations are not statistically significant. Another argument against the orbital modulation of the paleointensity is that it could be an artifact caused by paleoclimatically induced rock-magnetic changes in sediments [*Kok*, 1999; *Guyodo et al.*, 2000].

[5] In this paper, we present a stacked paleointensity record from 0.8 to 3 Ma using six sediment cores from the equatorial Pacific, three from the West Caroline Basin and three from the Manihiki Plateau (Figure 1). We show magnetic properties of the sediments are suitable for relative paleointensity estimation: little change in proxies of magnetic grain size and mineralogy. We compare our record with other published records of older than the Brunhes-Matuyama (B/M) boundary, and examine reproducibility of the "asymmetric sawtooth pattern." We also study possible existence of the orbital eccentricity frequency in paleointensity variations during the Matuyama and late Gauss Chrons.

## 2. Sampling and Measurements

[6] Three long piston cores taken from the West Caroline Basin in the western equatorial Pacific during the IMAGES IV campaign were used in this study (Figure 1 and Table 1). Results of core MD982187 are documented here for the first time, and those of other two cores, MD982183 and MD982185, were already reported by *Yamazaki and Oda* [2002, 2004]. The water depth of the site of MD982187, about 4600 m, is close to the carbonate compensation depth (CCD) in this area at present [*Berger et al.*, 1976]. The core consists mainly of hemipelagic clay with calcareous and siliceous microfossils, which is similar to those of MD982183 and MD982185. The sedimentation rate of MD982187 is 5 to 20 m/m.y. as shown later, which is lower than those of other two cores. This would reflect a larger distance of this site from New Guinea Island. Samples for paleomagnetic measurements were taken in 2002 from split core sections using plastic cubes of 7 $cm^3$.

[7] Three piston cores of 14 to 18 m long were taken from the Manihiki Plateau, central Pacific,

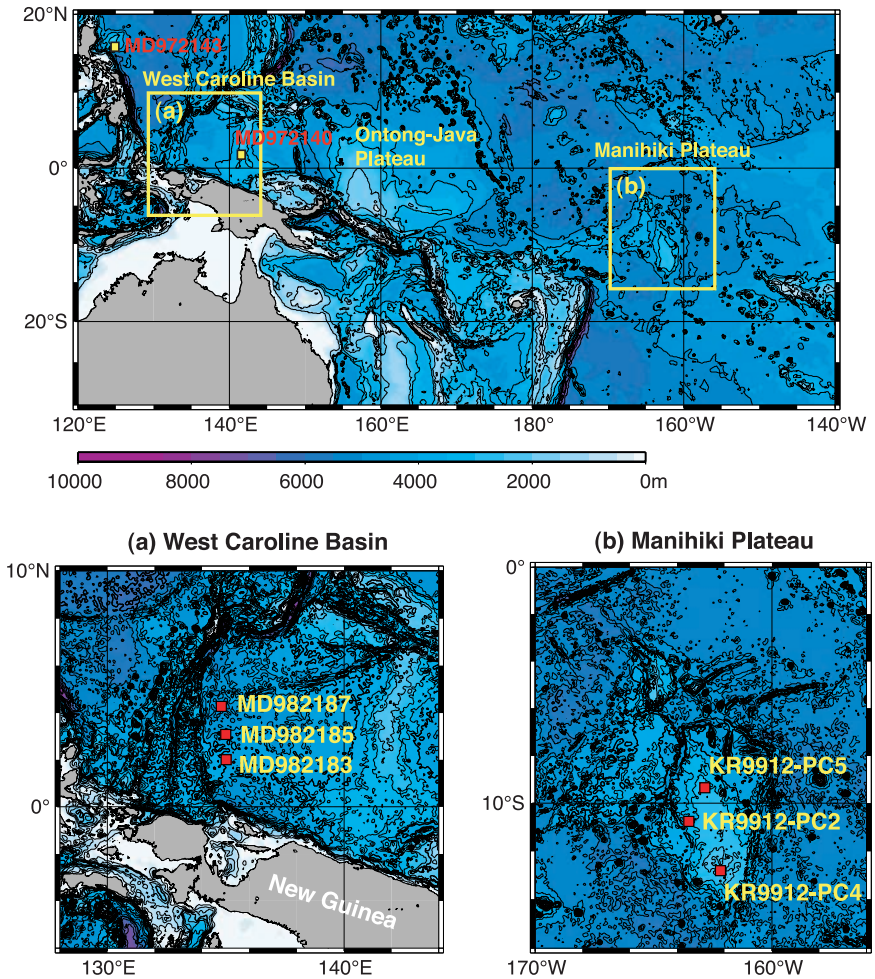


**Figure 1.** Location of sediment cores in (a) the West Caroline Basin and (b) the Manihiki Plateau utilized in this study.

during the KR99-12 cruise of R/V *Kairei* (Figure 1 and Table 1). Water depths of the coring sites range from about 2300 to 3400 m, which are shallower than the present CCD. The cores consist of calcareous ooze [*Yamada et al.*, 2000]. Sedimentation rates on the Manihiki Plateau are low in general, 3 to 15 m/m.y., because this area is off the high productivity province along the equator. Samples for paleomagnetic measurements were taken onboard in 2000 from split core sections using u-channels of 1 m long with a cross section of $2 \times 1.8$ cm$^2$ (cores KR9912-PC2 and KR9912-PC4) or discrete cubic samples of 7 cm$^3$ (core KR9912-PC5).

**Table 1.** Sediment Cores Used in This Study

| Core | Position | Depth, m | Core Length, m | Reference[a] |
|---|---|---|---|---|
| | | *West Caroline Basin* | | |
| MD982183 | 2°00.82′N, 135°01.26′E | 4388 | 36.8 | 1 |
| MD982185 | 3°05.05′N, 134°59.82′E | 4415 | 41.9 | 2 |
| MD982187 | 4°15.98′N, 134°49.11′E | 4623 | 29.9 | |
| | | *Manihiki Plateau* | | |
| KR9912-PC2 | 10°45.00S, 163°29.30′W | 3383 | 14.4 | |
| KR9912-PC4 | 12°48.08′S, 162°10.13′W | 2326 | 14.2 | |
| KR9912-PC5 | 9°21.01′S, 162°50.03′W | 2933 | 17.3 | |

[a] References: 1, *Yamazaki and Oda* [2004]; 2, *Yamazaki and Oda* [2002].

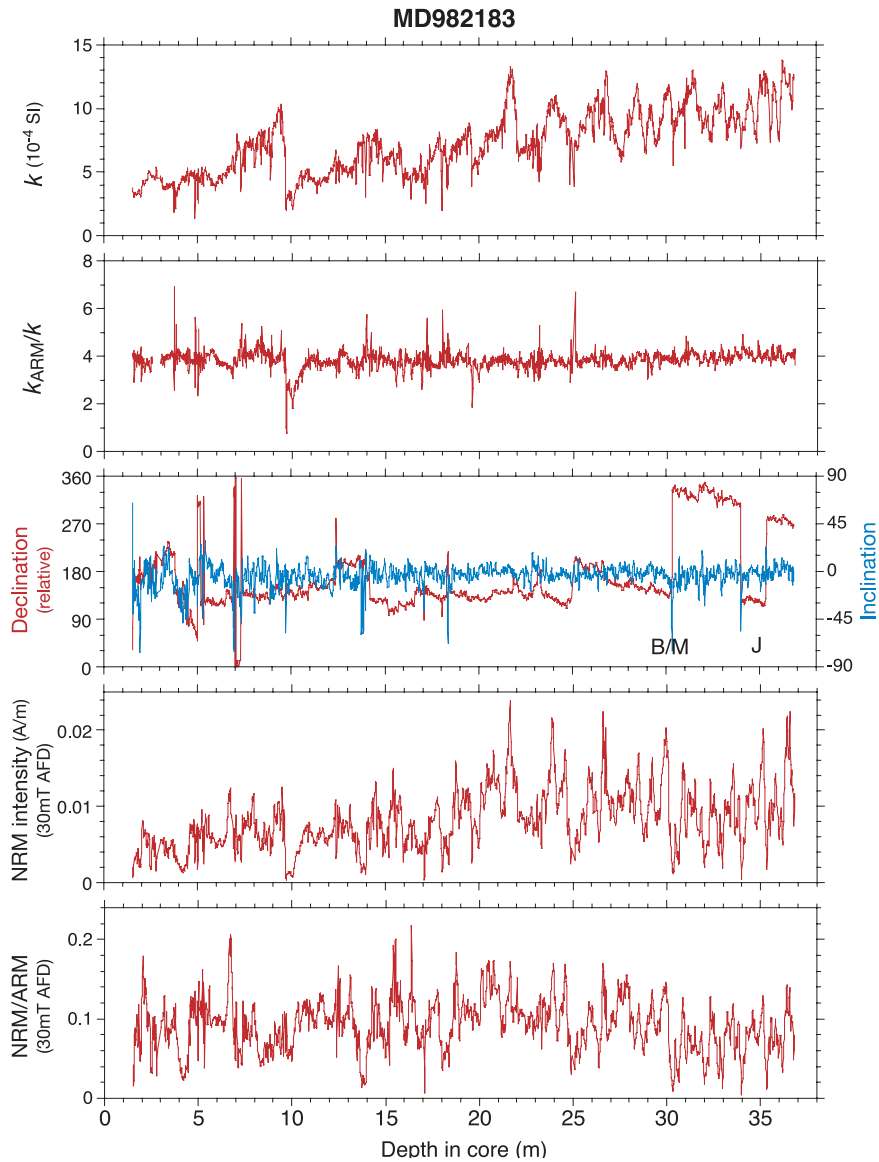


**Figure 2.** Remanent magnetization and magnetic properties of core MD982183. From the top panel, magnetic susceptibility ($k$), ratio of anhysteretic remanent magnetization (ARM) susceptibility to $k$, natural remanent magnetization (NRM) direction (red: relative declination, blue: inclination), NRM intensity, and NRM intensity normalized by ARM. B/M, Brunhes-Matuyama boundary; J, Jaramillo Subchron. Parts of the data were already reported by *Yamazaki and Oda* [2004].

[8] Remanent magnetization was measured with a cryogenic magnetometer system (2G Enterprises model 760R) with an in-line alternating-field (AF) demagnetizer. For u-channel samples, measurements were done at 1 cm intervals. The bore diameter of the magnetometer is 7.6 cm. Stepwise AF demagnetization up to 80 mT was performed on natural remanent magnetization (NRM). Anhysteretic remanent magnetization (ARM) was imparted by superimposing a DC biasing field of 0.1 mT on a smoothly decreasing AF with a peak field of 80 mT. Isothermal remanent magnetization (IRM) was given by pulse magnetizers. IRM of discrete samples was measured using a spinner magnetometer (Natsuhara-Giken SMM-85). First, IRM was imparted at 2.5T for discrete samples, and 0.8T for u-channels (the maximum field of our instrument for u-channels). Then, IRM of 0.3T was successively imparted in the direction opposite to the initial IRM. S ratio ($S_{-0.3T}$) was calculated according to the definition of *Bloemendal et al.* [1992]. To increase the resolution of the records,

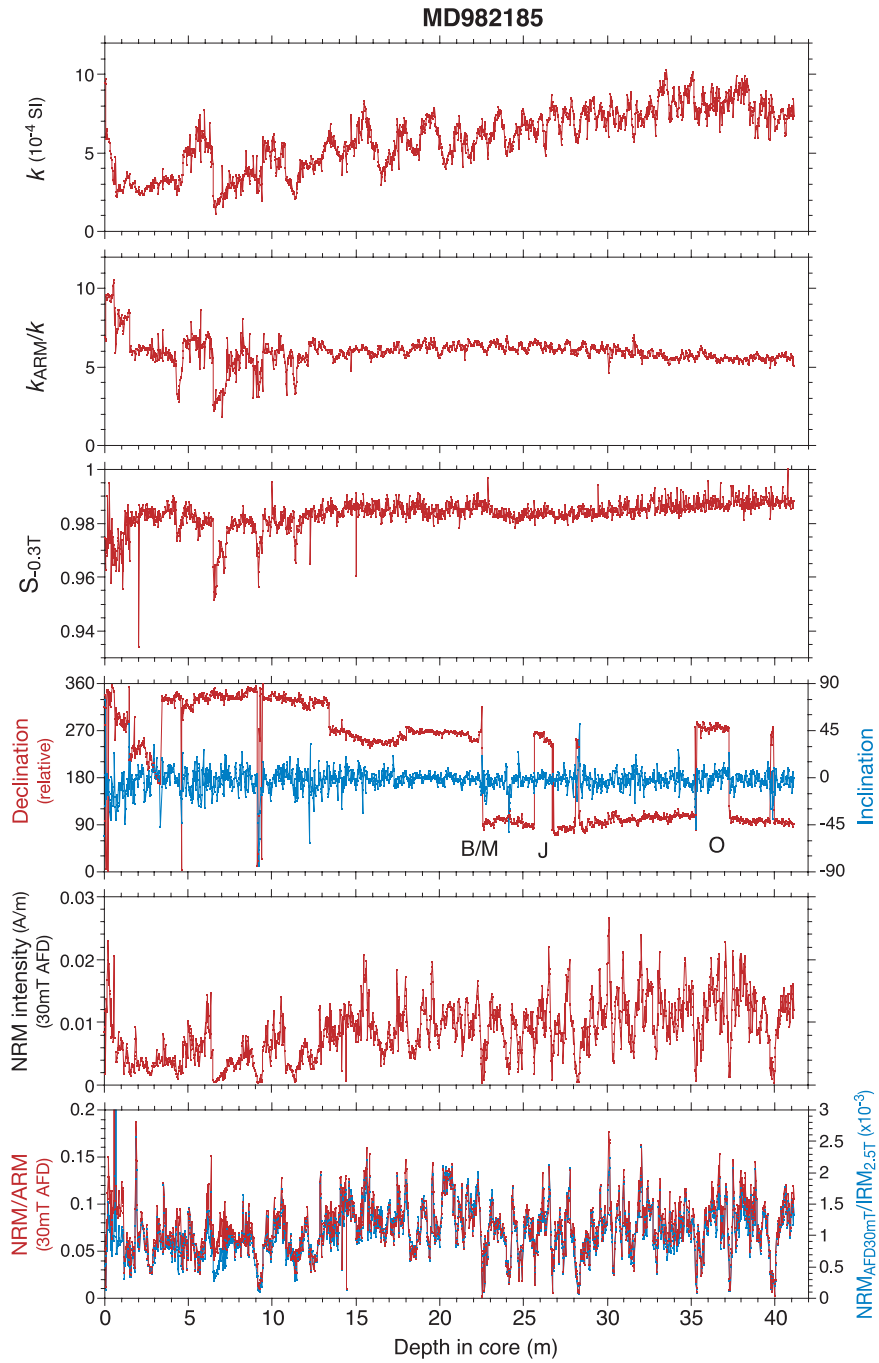


**Figure 3.** Remanent magnetization and magnetic properties of core MD982185. From the top panel, magnetic susceptibility ($k$), ratio of ARM susceptibility to $k$, S ratio ($S_{-0.3T}$), NRM direction (red: relative declination, blue: inclination), NRM intensity, and NRM intensity normalized by ARM (red) and isothermal remanent magnetization (IRM) (blue). B/M, Brunhes-Matuyama boundary; J, Jaramillo Subchron; O, Olduvai Subchron. Parts of the data were already reported by *Yamazaki and Oda* [2002].

the deconvolution procedure of *Oda and Shibuya* [1996] was applied to the u-channel data: NRM data for each demagnetization step, and the ARM and IRM data. Spatial resolution after the deconvolution is considered to be about 2 cm, close to the measurements using discrete samples.

[9] Stepwise AF demagnetization showed that remanent magnetization of most samples consists of a single component except for the first few demagnetization steps. Magnetic overprint of probably viscous remanent magnetization (VRM) origin could be removed by AF up to 20 mT in

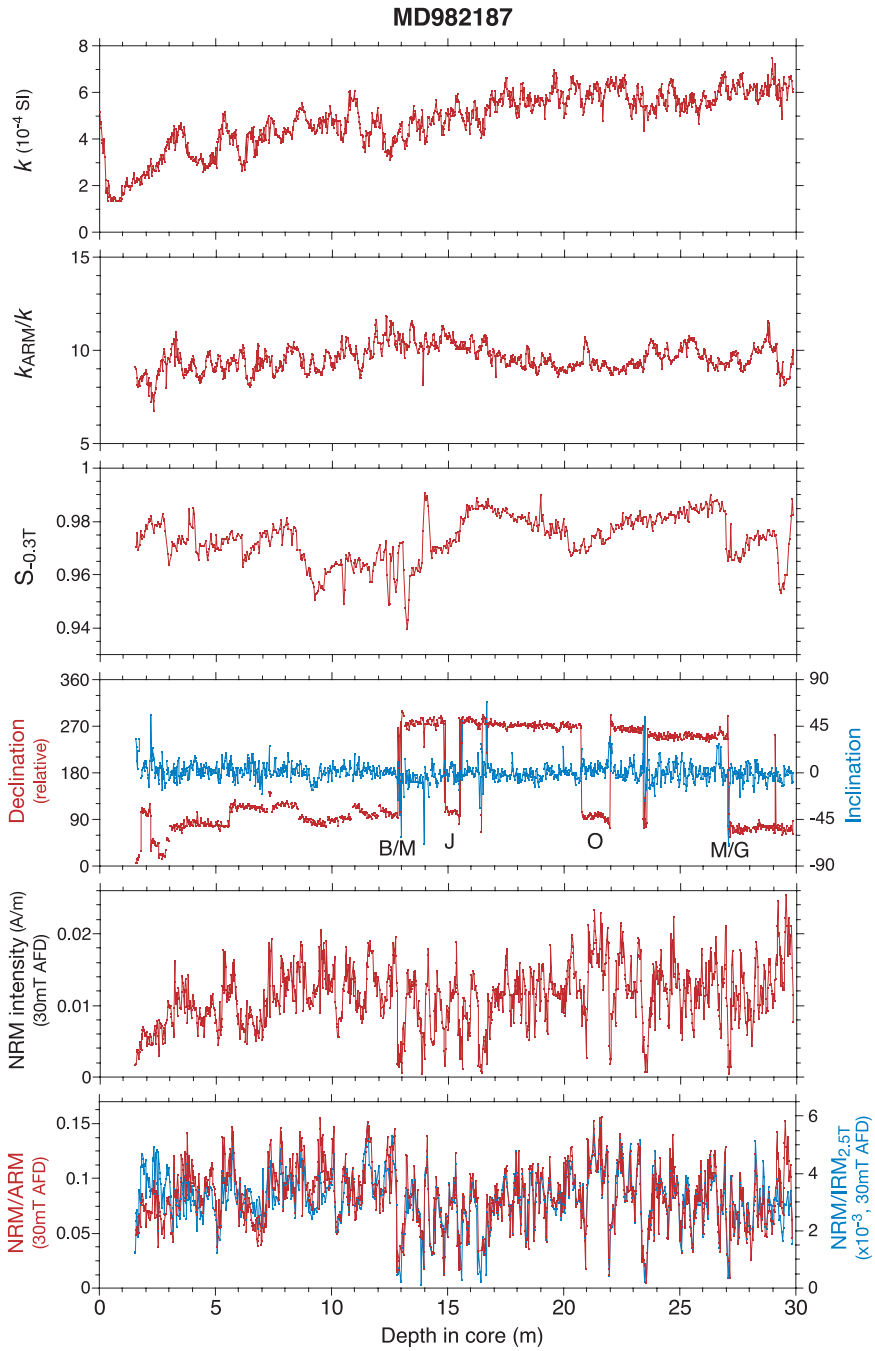


**Figure 4.** Remanent magnetization and magnetic properties of core MD982187. From the top panel, magnetic susceptibility ($k$), ratio of ARM susceptibility to $k$, S ratio ($S_{-0.3T}$), NRM direction (red: relative declination, blue: inclination), NRM intensity, and NRM intensity normalized by ARM (red) and IRM (blue). B/M, Brunhes-Matuyama boundary; J, Jaramillo Subchron; O, Olduvai Subchron; M/G, Matuyama-Gauss boundary.

general. Some samples from polarity boundaries or excursions required stronger AF fields to remove magnetic overprints. In an exceptional case, no stable component was isolated by the AF demagnetization, and such samples were excluded from further analyses. Directions of NRM were determined by applying the principal component analysis (PCA) [*Kirschvink*, 1980]. The maximum angular deviations (MADs) of hemipelagic clay samples from the West Caroline Basin are 1° to 2° except for polarity transitions and excursions. The MADs are a little larger, 2° to 5°, for calcareous ooze from the Manihiki Plateau.

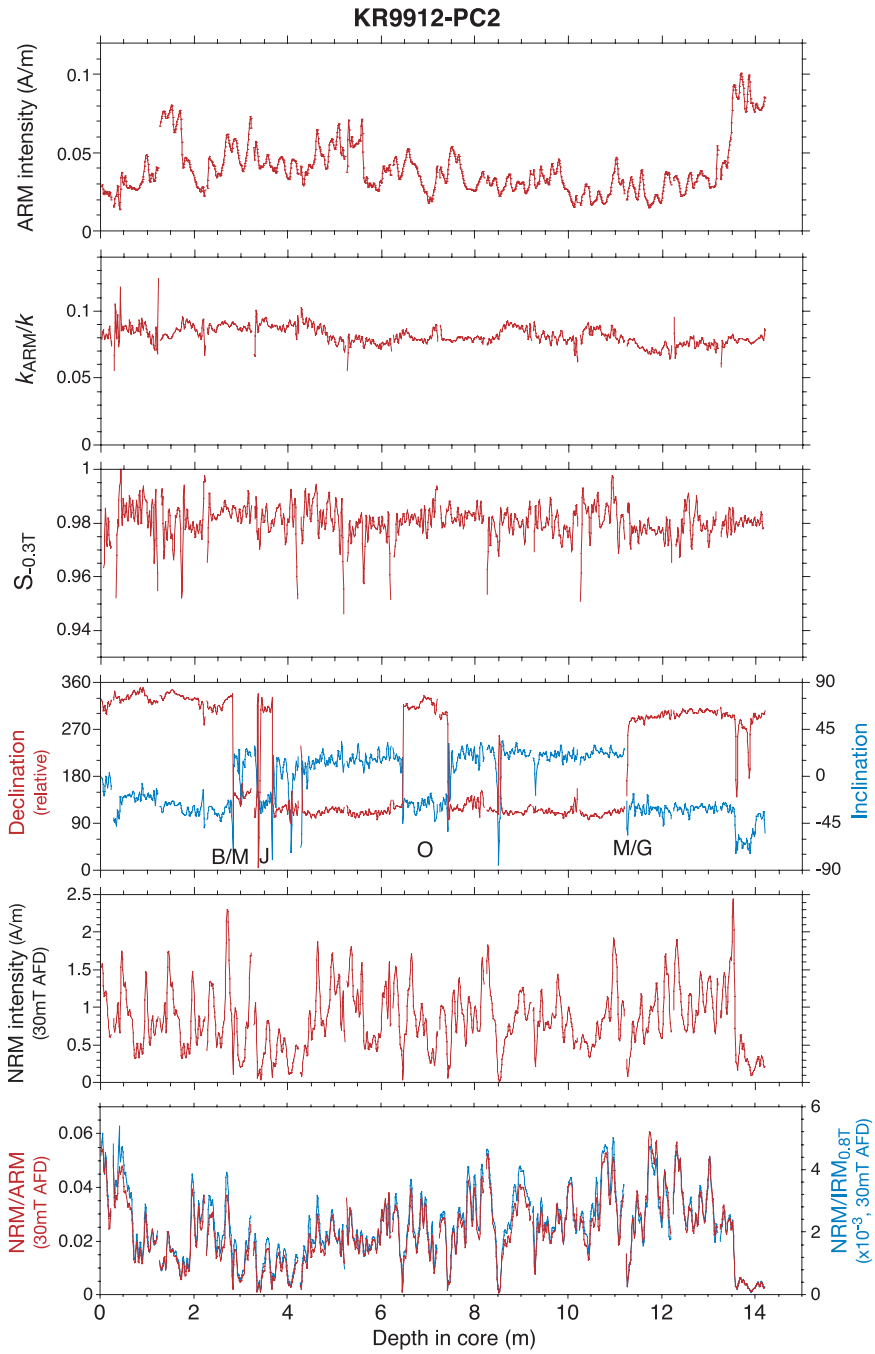


**Figure 5.** Remanent magnetization and magnetic properties of core KR9912-PC2. From the top panel, ARM, ratio of ARM to IRM, S ratio ($S_{-0.3T}$), NRM direction (red: relative declination, blue: inclination), NRM intensity, and NRM intensity normalized by ARM (red) and IRM (blue). B/M, Brunhes-Matuyama boundary; J, Jaramillo Subchron; O, Olduvai Subchron; M/G, Matuyama-Gauss boundary.

[10] Magnetic susceptibility ($k$) of discrete samples was measured using a KappaBridge KLY 3. Magnetic susceptibility of u-channels was measured at 1 cm intervals using a Bartington Instruments MS2 susceptometer with a loop sensor of 4.5 cm in diameter. The deconvolution procedure of *Oda and Shibuya* [1994] was applied to the data of MD982183. The resolution of the susceptibility data from the u-channels of KR9912-PC2 and KR9912-PC4 was too low for applying deconvolution because their magnetic susceptibilities were very low ($\sim 1 \times 10^{-5}$ SI), reflecting high carbonate contents of the sediments on the Manihiki Plateau. For these cores, ARM

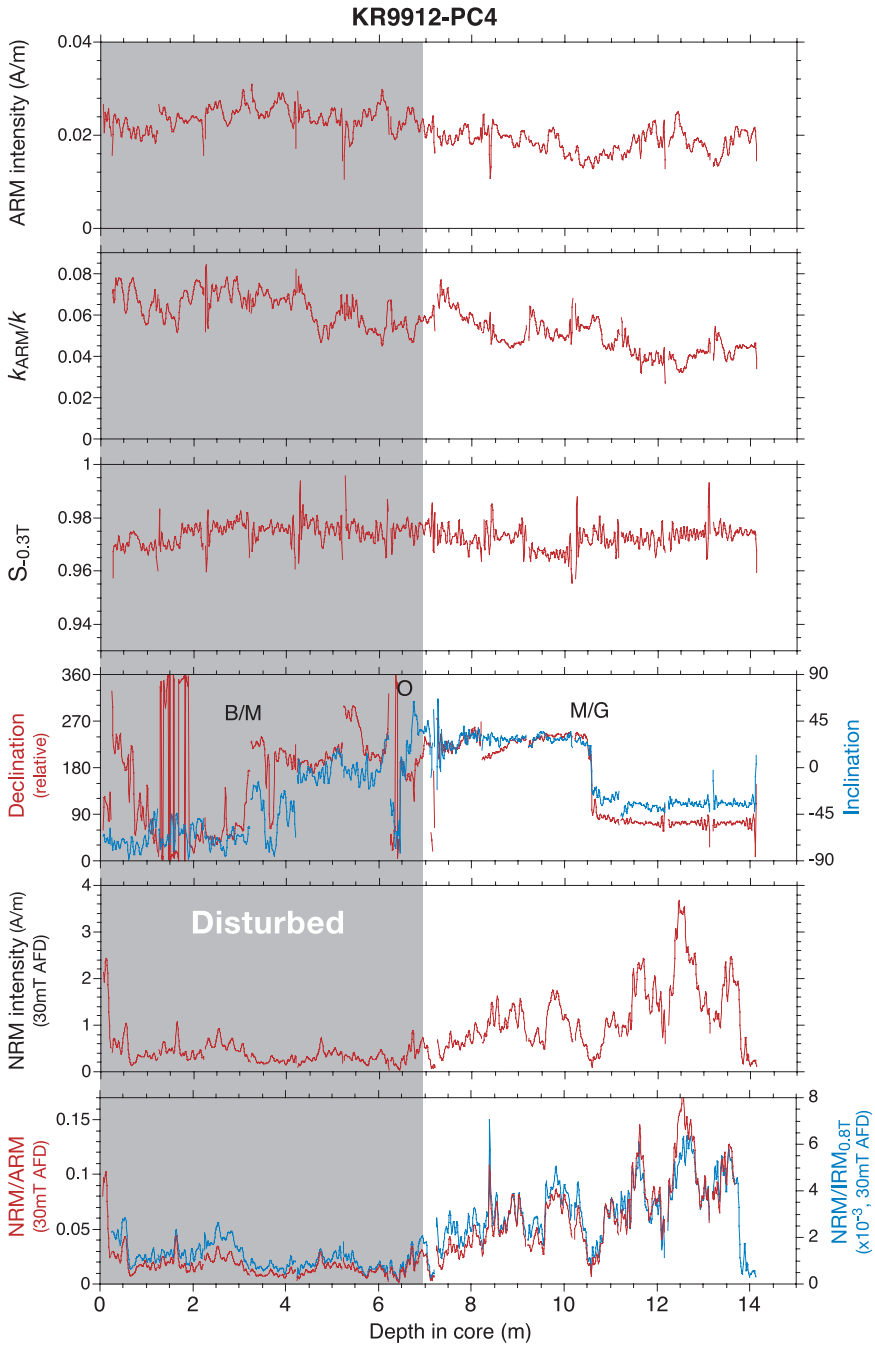


**Figure 6.** Remanent magnetization and magnetic properties of core KR9912-PC4. From the top panel, ARM, ratio of ARM to IRM, S ratio ($S_{-0.3T}$), NRM direction (red: relative declination, blue: inclination), NRM intensity, and NRM intensity normalized by ARM (red) and IRM (blue). B/M, Brunhes-Matuyama boundary; J, Jaramillo Subchron; O, Olduvai Subchron; M/G, Matuyama-Gauss boundary. The upper 7 m of the core was physically disturbed (shaded in gray).

was instead used for a magnetic concentration parameter.

## 3. Results

[11] Figures 2 through 7 display results of paleomagnetic and rock-magnetic measurements of each core: magnetic concentration ($k$ or ARM), a magnetic grain-size proxy ($k_{ARM}/k$ or ARM/IRM), a magnetic mineralogy proxy ($S_{-0.3T}$), NRM direction and intensity, and normalized intensity (NRM/ARM and NRM/IRM). For the normalized intensity, NRM and the normalizers after AF demagnetization of 30 mT were adopted. Almost identical

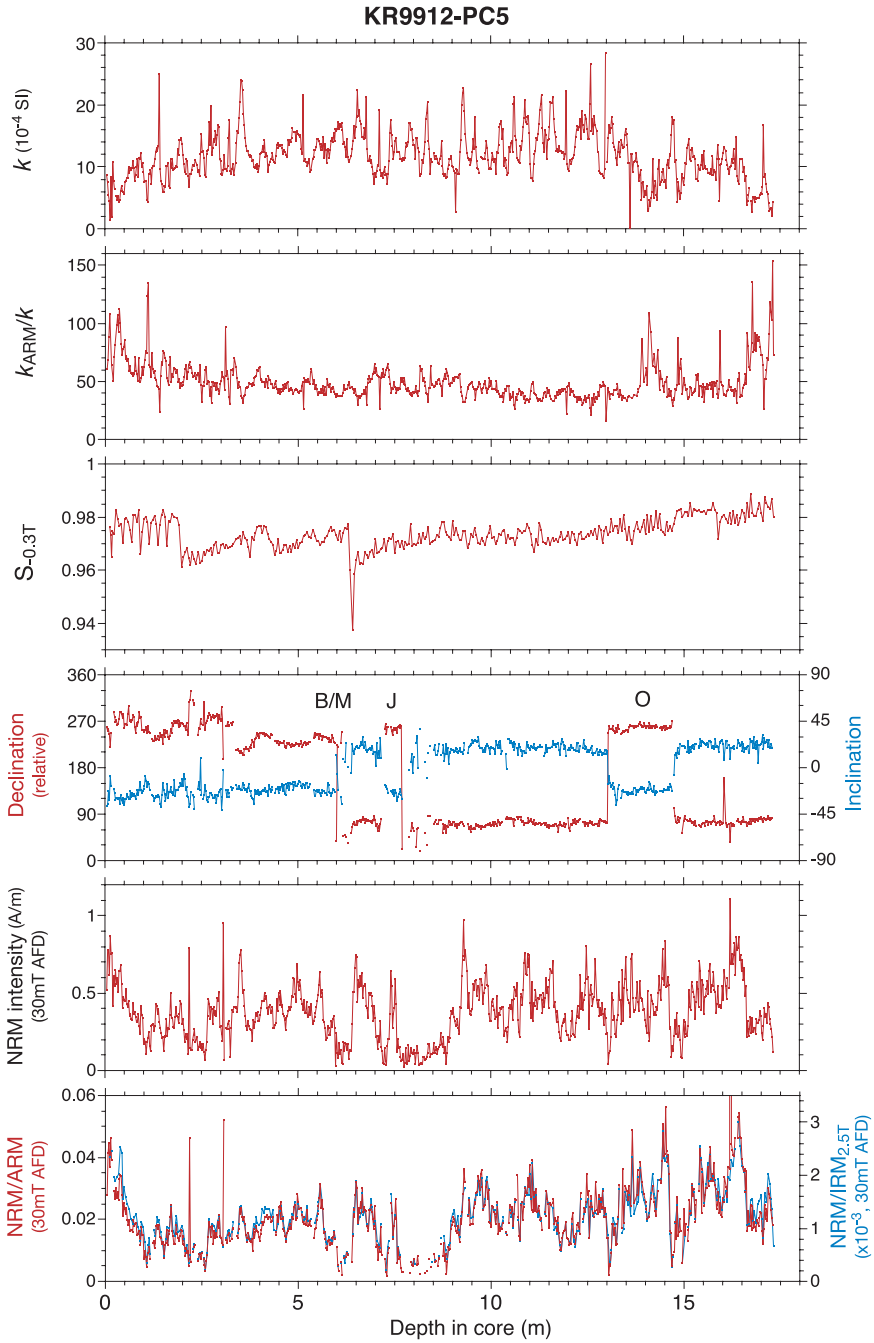


**Figure 7.** Remanent magnetization and magnetic properties of core KR9912-PC5. From the top panel, magnetic susceptibility ($k$), ratio of ARM susceptibility to $k$, S ratio ($S_{-0.3T}$), NRM direction (red: relative declination, blue: inclination), NRM intensity, and NRM intensity normalized by ARM (red) and IRM (blue). B/M, Brunhes-Matuyama boundary; J, Jaramillo Subchron; O, Olduvai Subchron.

results were obtained by AF demagnetization of 20 mT.

## 3.1. West Caroline Basin

[12] All three cores from the West Caroline Basin show clear magnetic polarity sequences, and on the basis of the magnetostratigraphy the age of the bottom of each core is estimated to be about 1.2 Ma for MD982183 (Figure 2), 2.2 Ma for MD982185 (Figure 3), and 3.0 Ma for MD982187 (Figure 4). The Cobb Mountain Subchron (1.201–1.211 Ma, *Cande and Kent* [1995]) and the Reunion Subchron (2.115–

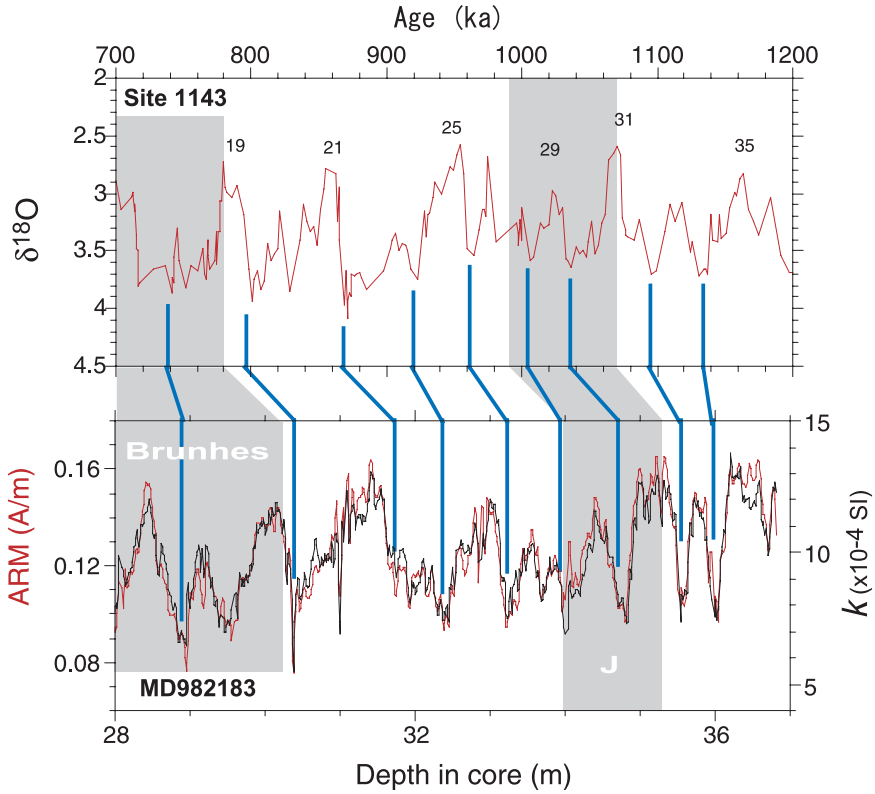


**Figure 8.** Age control of MD982183. Magnetic concentration variation (red: ARM, black: magnetic susceptibility $k$) is correlated to the oxygen isotope ($\delta^{18}O$) curve of ODP Site 1143 in the South China Sea [*Tian et al.*, 2002] at the horizons indicated by tie lines. Magnetic polarity is shown by graying normal polarity zones. Ages of the polarity boundaries in the panel of the $\delta^{18}O$ curve are after *Cande and Kent* [1995], and observed depths of polarity boundaries are displayed in the panel of magnetic concentration. Marine isotope stage (MIS) numbers are attached to the $\delta^{18}O$ curve. J, Jaramillo Subchron.

2.153 Ma [*Channell et al.*, 2003]) are recognized in MD982185 and MD982187. Directional fluctuations with low remanent intensities at about 24 m in depth of MD982185 and 14.5 m of MD982187 would correspond to the Kamikatsura excursion (0.886 Ma [*Singer et al.*, 1999]).

[13] It is known that variations in $k$ mimic the oxygen isotope ($\delta^{18}O$) curve in the West Caroline Basin [*Yamazaki and Ioka*, 1994; *Yamazaki and Oda*, 2002]. Glacial-interglacial changes of carbonate production and/or preservation cause cyclic variations in carbonate content of the sediments, and $k$ fluctuates due to a dilution effect by carbonates. Higher carbonate content and lower $k$ occur in glacial periods, which is the general pattern in the Pacific [*Archer et al.*, 2000]. The susceptibility variations of MD982187 as well as MD982183 and MD982185 follow this pattern, and these are utilized for age control of the cores as shown later.

[14] S ratios ($S_{-0.3T}$) of MD982185 are high and very uniform, 0.98 to 0.99, except for the upper part of the core. Core MD982187 also shows high and uniform S ratios, although variations are slightly larger, ranging from 0.95 to 0.99. These results indicate that remanent magnetization in the West Caroline Basin sediments is carried by low-coercivity magnetic minerals like magnetite, and magnetic mineralogy does not vary significantly with depth of the cores. The high and uniform S ratios suggest that reductive dissolution of magnetites did not occur in these sediments. It is expected that magnetite dissolution accompanies a remarkable decrease in S ratios because high-coercivity minerals like hematite are more resistive to reduction diagenesis [*Yamazaki et al.*, 2003]. We infer that magnetic mineralogy of MD982183 would be similar to other two cores, although we could not obtain S ratios because IRMs of the u-channel samples were too strong to be measured by the cryogenic magnetometer.

[15] All three cores show little downcore variation in the magnetic grain-size proxy ($k_{ARM}/k$) except for the upper part of MD982183 and MD982185,

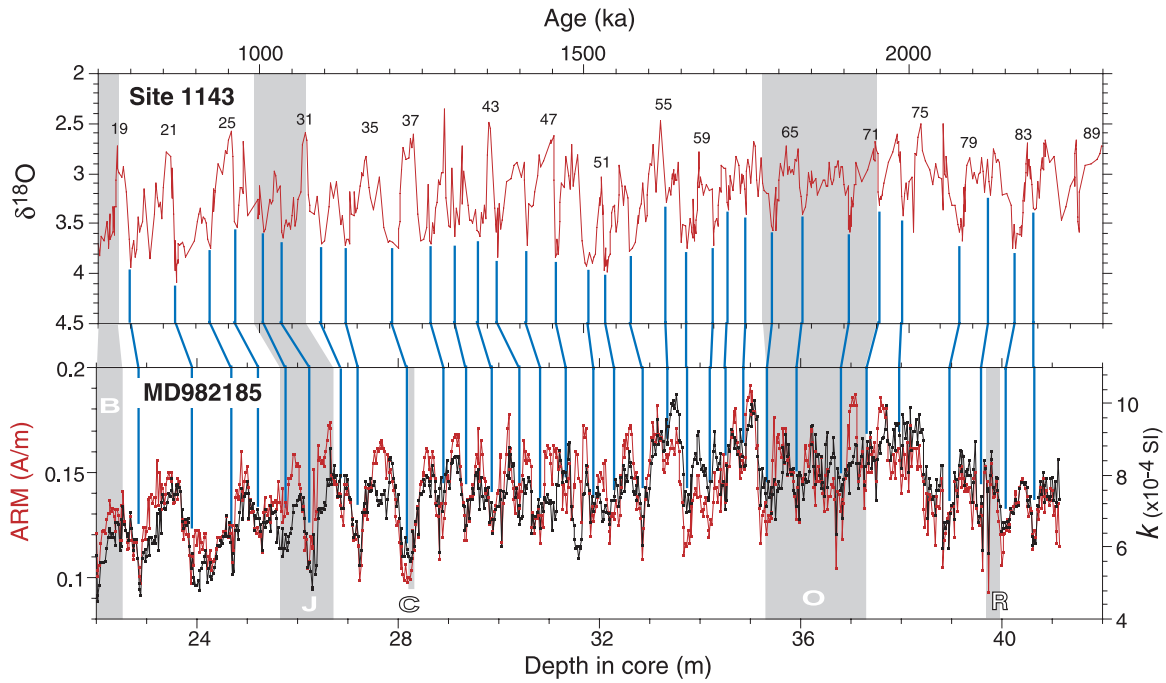


**Figure 9.** Age control of MD982185. Magnetic concentration variation (red: ARM, black: $k$) is correlated to the $\delta^{18}O$ curve of ODP Site 1143 in the South China Sea [*Tian et al.*, 2002] at the horizons indicated by tie lines. Magnetic polarity is shown by graying normal polarity zones. Ages of the polarity boundaries in the panel of the $\delta^{18}O$ curve are after *Cande and Kent* [1995], and observed depths of polarity boundaries are displayed in the panel of magnetic concentration. MIS numbers are attached to the $\delta^{18}O$ curve. B, Brunhes Chron; J, Jaramillo Subchron; C, Cobb Mountain Subchron; O, Olduvai Subchron; R, Reunion Subchron.

indicating uniform magnetic grain size. The average of $k_{ARM}/k$ of MD982187 is larger than those of other two cores, suggesting finer magnetic grain size of MD982187. This would reflect the larger distance of the site from New Guinea Island, from which magnetic minerals may have been supplied.

## 3.2. Manihiki Plateau

[16] All three cores from the Manihiki Plateau have low magnetic susceptibility ($\sim 10^{-5}$ SI) and weak NRM intensity ($10^{-3}$ to $10^{-4}$ A/m) in general, which reflects the lithology of the cores, that is, calcareous ooze. Variations of magnetic concentration represented by $k$ or ARM contain short-wavelength components on the order of few tens of centimeters, which is particularly remarkable for KR9912-PC5 (Figure 7). They are correlated with glacial-interglacial cycles as shown later.

### 3.2.1. KR9912-PC2

[17] The magnetic polarity sequence of NRM indicates that the age of the bottom of the core is about 3 Ma, and that the sedimentation rate decreases upward (Figure 5). A fluctuation of NRM directions at 8.5 m in depth with a intensity drop would be a manifestation of the Reunion Subchron. Unstable declinations with anomalously steep inclinations below 13.6 m may correspond to the Kaena Subchron. Alternatively, a hiatus may have occurred at this horizon. A sudden downward increase in magnetic concentration (ARM) at this depth suggests a different sedimentary environment with an age gap. S ratios are higher than 0.97 in general, implying that the NRM is carried by magnetite throughout the core. The magnetic grain-size proxy (ARM/IRM) shows little variation throughout the core, indicating uniform grain size.

### 3.2.2. KR9912-PC4

[18] The magnetic polarity sequence shows that the core reaches the Gauss Chron (Figure 6). We consider that the upper half of the core was physically disturbed during coring, which would have caused anomalous inclination values. This core consists of loose sandy foraminiferal ooze, and sediments of such lithology would easily suffer disturbance. The lower half of the core is, on the other hand, considered to be in a good condition, judging from the observation that NRM directions before and after the M/G boundary are almost

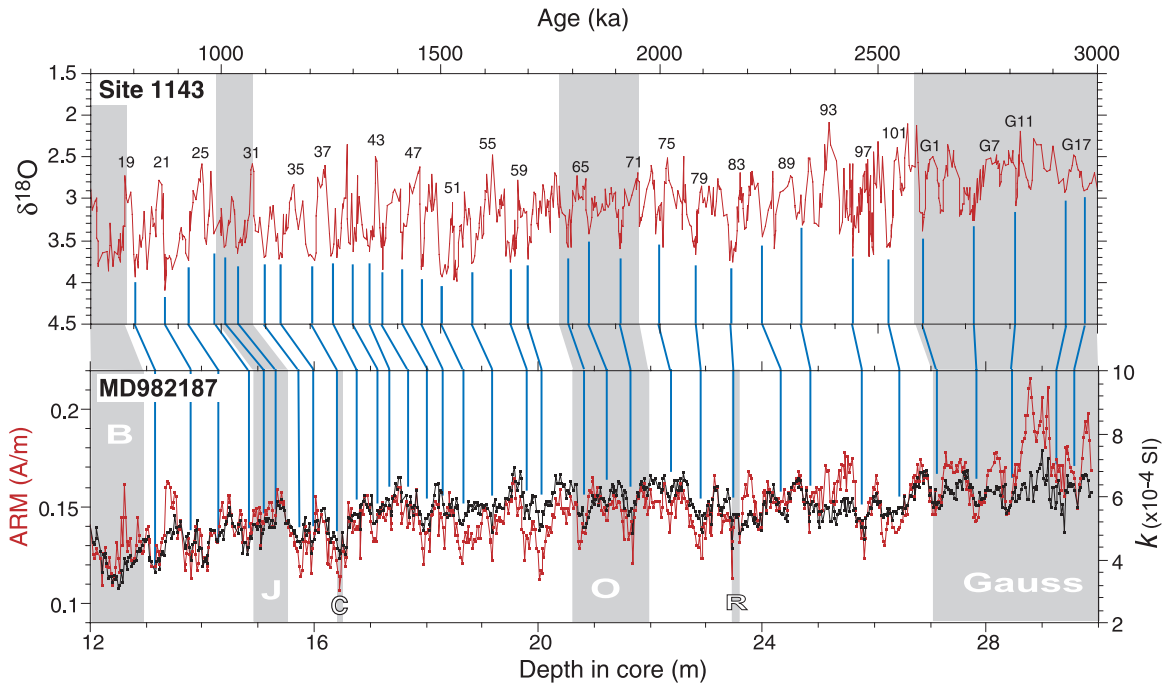


**Figure 10.** Age control of MD982187. Magnetic concentration variation (red: ARM, black: $k$) is correlated to the $\delta^{18}O$ curve of ODP Site 1143 in the South China Sea [*Tian et al.*, 2002] at the horizons indicated by tie lines. Magnetic polarity is shown by graying normal polarity zones. Ages of the polarity boundaries in the panel of the $\delta^{18}O$ curve are after *Cande and Kent* [1995], and observed depths of polarity boundaries are displayed in the panel of magnetic concentration. MIS numbers are attached to the $\delta^{18}O$ curve. B, Brunhes Chron; J, Jaramillo Subchron; C, Cobb Mountain Subchron; O, Olduvai Subchron; R, Reunion Subchron.

antipodal. The sedimentation rate of the lower part of the core is much higher than the upper part. The high and constant S ratios, between 0.96 and 0.98, show that magnetic minerals of this core is also dominated by magnetite. The ratios of ARM to IRM show some variations, and an inverse correlation between ARM/IRM and magnetic concentration (ARM) can be recognized; for example, an increasing trend of ARM/IRM from 10.5 to 12.5 m in depth corresponds to a decrease in ARM, and vise versa from 12.5 to 13.5 m. This suggests that the variations in ARM/IRM of this core are partly controlled by magnetic interaction among grains, and may not necessarily reflect magnetic grain size changes [*Yamazaki and Ioka*, 1997]. ARM is known to be quite sensitive to the magnetic interaction [e.g., *Sugiura*, 1979].

### 3.2.3. KR9912-PC5

[19] The age of the bottom of the core is estimated to be 2.2 Ma from the magnetostratigraphy (Figure 7). NRMs between 7.7 and 8.5 m in depth were not stable; a primary magnetization component could not be isolated by stepwise AF demagnetization. The samples below 8.5 m are used hereafter for paleointensity estimation. This core also shows a downcore increase in sedimentation rate. The S ratios ranging from 0.96 to 0.99 again indicate the dominance of magnetite as a carrier of NRM. The magnetic grain-size proxy, $k_{ARM}/k$, shows an inverse correlation with magnetic concentration ($k$): long-term decreasing trends in $k_{ARM}/k$ from the top to 7 m and 7.5 to 13.5 m in depth correspond to increasing trends in $k$, and a peak in $k_{ARM}/k$ at about 14.0 m coincides with a low in $k$. This is similar to the case of KR9912-PC4, and suggests that magnetic concentration rather than magnetic grain size controls the parameter.

## 4. Age Control

[20] High-resolution age control of the sediment cores was performed by correlating magnetic concentration ($k$ and/or ARM) variations to the $\delta^{18}O$ stratigraphy (Figures 8 through 13). For the cores from the Manihiki Plateau, color reflectance data were also used in addition to the magnetic concentration. The $\delta^{18}O$ curve from ODP Site 1143 in the South China Sea [*Tian et al.*, 2002] was used as a target curve of the cores in the West Caroline Basin, because the two areas are geographically nearby. For the cores from the Manihiki Plateau, the global

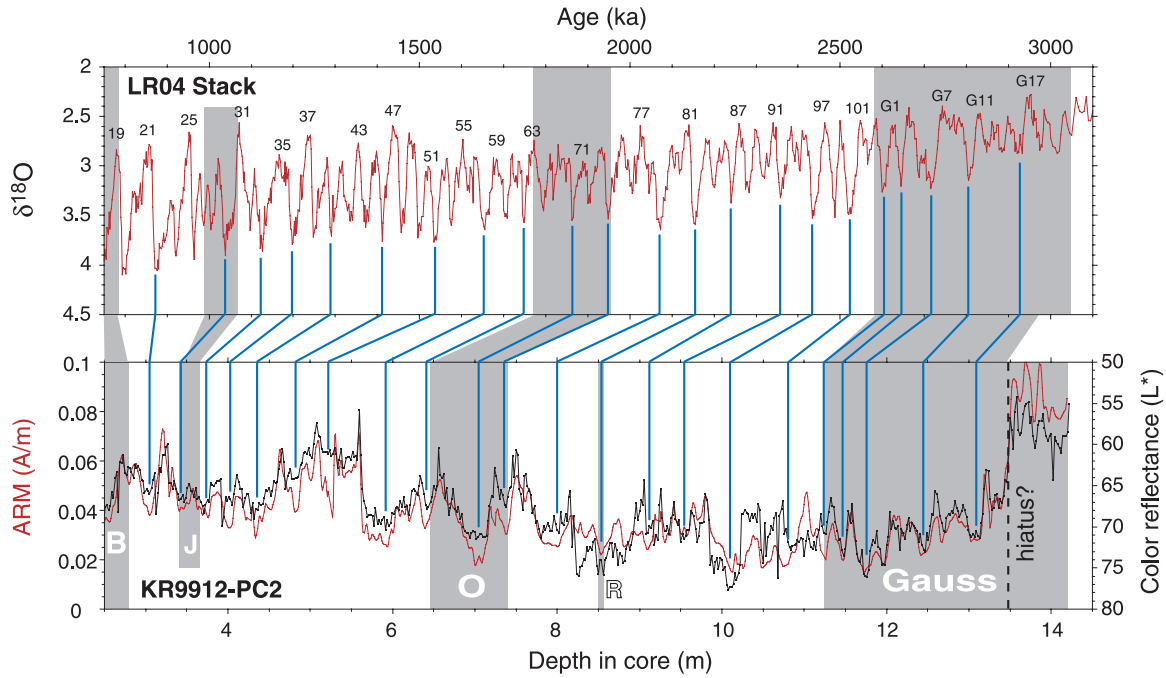


**Figure 11.** Age control of KR9912-PC2. Magnetic concentration variation represented by ARM (red) and color reflectance (L*) (black) is correlated to the global $\delta^{18}O$ stack LR04 [*Lisiecki and Raymo*, 2005] at the horizons indicated by tie lines. Magnetic polarity is shown by graying normal polarity zones. Ages of the polarity boundaries in the panel of the $\delta^{18}O$ curve are after *Cande and Kent* [1995], and observed depths of polarity boundaries are displayed in the panel of magnetic concentration. MIS numbers are attached to the $\delta^{18}O$ curve. B, Brunhes Chron; J, Jaramillo Subchron; O, Olduvai Subchron; R, Reunion Subchron.

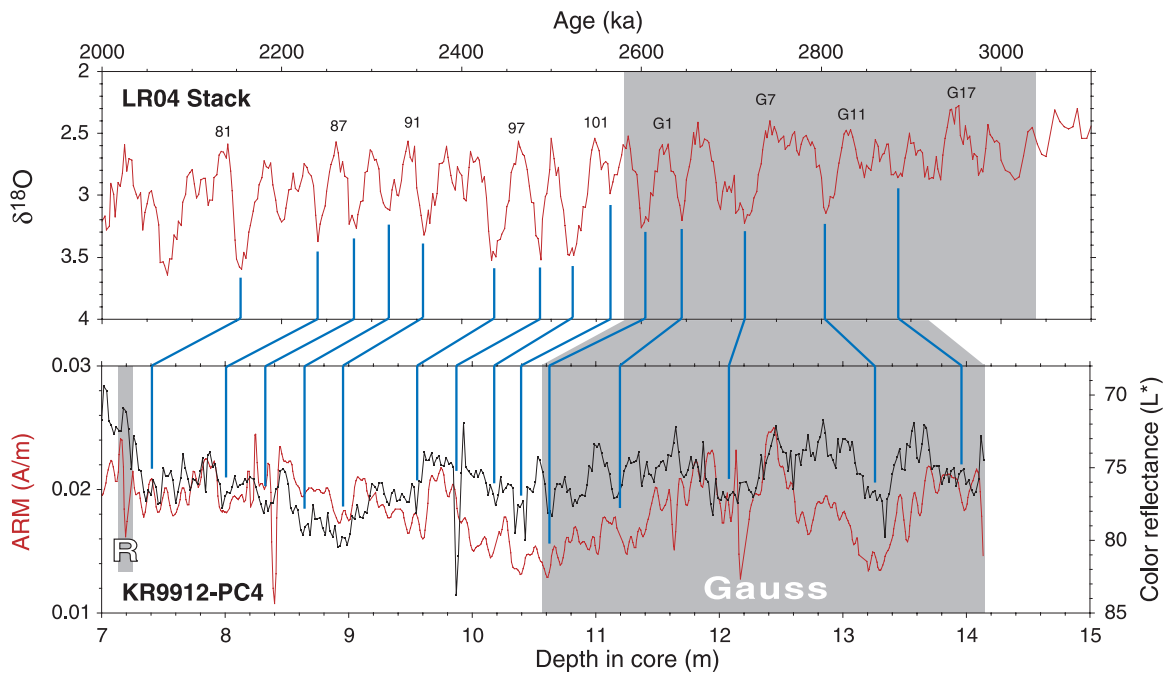


**Figure 12.** Age control of KR9912-PC4. Magnetic concentration variation represented by ARM (red) and color reflectance (L*) (black) is correlated to the global $\delta^{18}O$ stack LR04 [*Lisiecki and Raymo*, 2005] at the horizons indicated by tie lines. Magnetic polarity is shown by graying normal polarity zones. Ages of the polarity boundaries in the panel of the $\delta^{18}O$ curve are after *Cande and Kent* [1995], and observed depths of polarity boundaries are displayed in the panel of magnetic concentration. MIS numbers are attached to the $\delta^{18}O$ curve. R, Reunion Subchron.

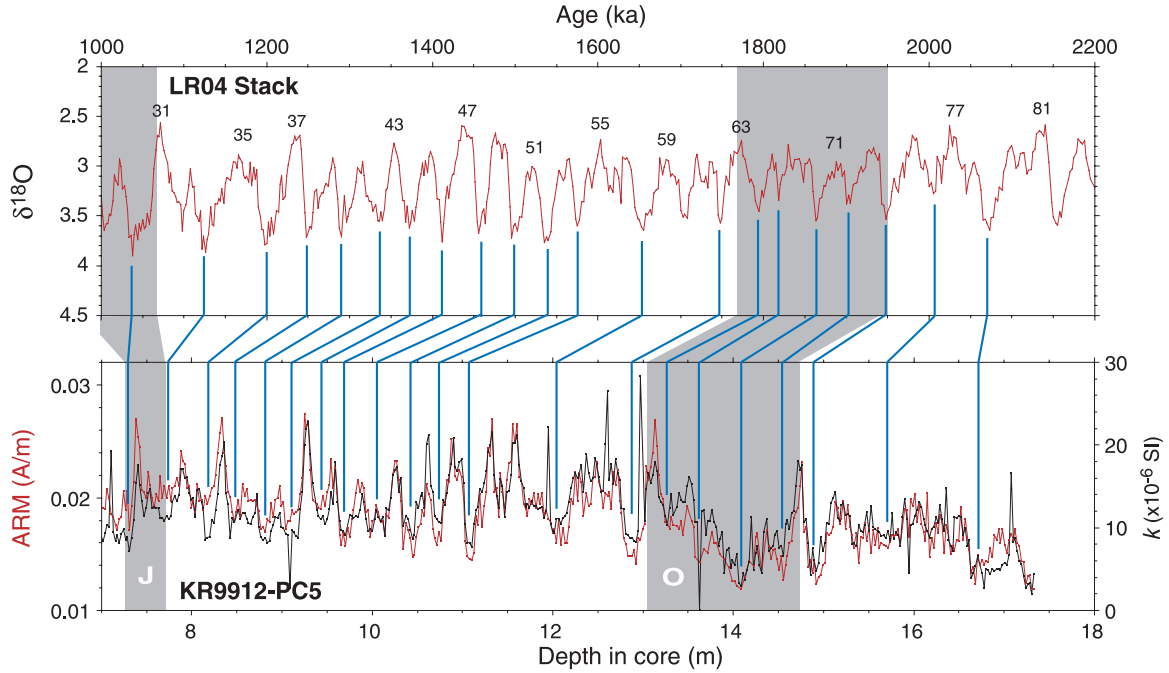


**Figure 13.** Age control of KR9912-PC5. Magnetic concentration variation (red: ARM, black: *k*) is correlated to the global $\delta^{18}$O stack LR04 [*Lisiecki and Raymo*, 2005] at the horizons indicated by tie lines. Magnetic polarity is shown by graying normal polarity zones. Ages of the polarity boundaries in the panel of the $\delta^{18}$O curve are after *Cande and Kent* [1995], and observed depths of polarity boundaries are displayed in the panel of magnetic concentration. MIS numbers are attached to the $\delta^{18}$O curve. J, Jaramillo Subchron; O, Olduvai Subchron.

$\delta^{18}$O stack LR04 [*Lisiecki and Raymo*, 2005] was used. These two $\delta^{18}$O curves have some differences in the shape of peaks and troughs, which would be probably due to reduced local effects by stacking in LR04. The two curves give almost identical ages after 3 Ma, although assignment of the marine isotope stage (MIS) numbers from MIS 65 to 77 is different (Figure 14).

[21] We first tied magnetic polarity boundaries to MISs using reported correspondence between them: the B/M boundary at MIS 19, the Jaramillo Subchron from MISs 28 to 31, the Olduvai Subchron from MISs 63 to 74 (LR04) or MISs 63 to 72 (ODP Site 1143) (Figure 14), and the M/G boundary at MIS 104 (In Table 4 of *Lisiecki and Raymo* [2005], MIS G2 is assigned to the M/G boundary, but their Figure 4 shows that the boundary occurs at MIS 104). Then, we tried to correlate the magnetic concentration variations to the $\delta^{18}$O curves between the polarity boundaries. We assigned glacial periods (troughs in the figures of the $\delta^{18}$O curves) to lows in the magnetic concentration, that is, higher carbonate contents in glacial periods known as the Pacific pattern. We assumed no time lag between the magnetic concentration and the $\delta^{18}$O curves.

[22] The variations in *k* and ARM of the cores from the West Caroline Basin closely resemble the target $\delta^{18}$O curve, and hence assignment of MISs was straightforward (Figures 8, 9, and 10). Uncertainty in age control of these cores is considered to be within one obliquity cycle (~40 kyr) in general. The age of KR9912-PC5 from the Manihiki Plateau is also relatively well constrained; the core shows clear peaks in ARM and *k* (Figure 13). On

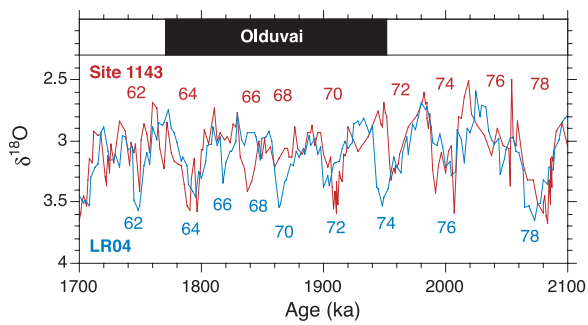


**Figure 14.** Difference in assignment of marine isotope stage (MIS) numbers around the Olduvai Subchron between the $\delta^{18}$O curves of ODP Site 1143 [*Tian et al.*, 2002] (red) and the LR04 stack [*Lisiecki and Raymo*, 2005] (black).

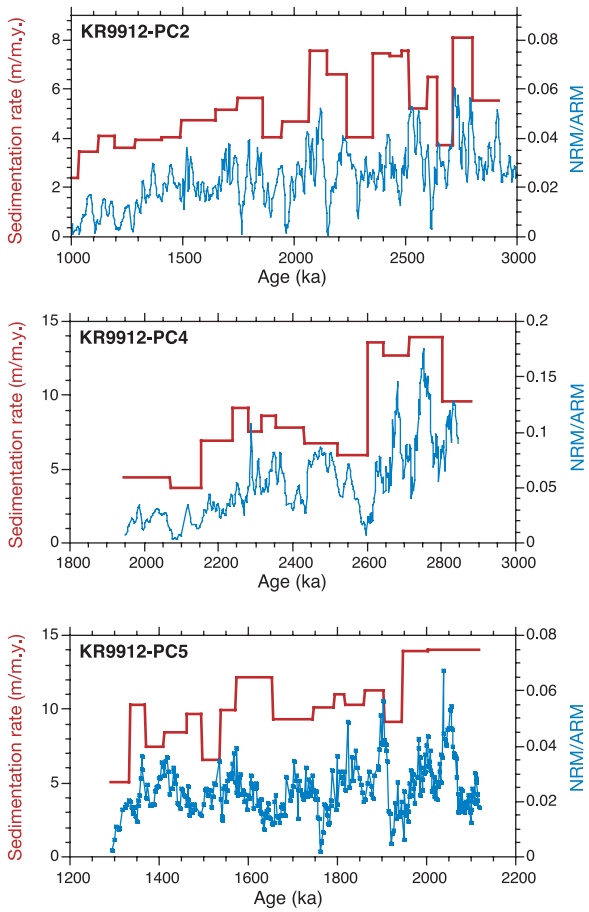


**Figure 15.** Upward decreases of normalized intensity (NRM/ARM) and sedimentation rate in the cores from the Manihiki Plateau. Sedimentation rate was calculated assuming a constant rate between tie points shown in Figures 11, 12, and 13.

the other hand, correlation between the magnetic concentration and the $\delta^{18}O$ is not obvious in other two cores from the Manihiki Plateau (Figures 11 and 12), partly because the magnetic concentrations have longer-wavelength changes as well as the variations on the order of tens of centimeters correlative with the ~40 kyr $\delta^{18}O$ cycles. For these cores, MIS assignments other than those shown in the figures are possible, and hence uncertainty in age control may be one obliquity cycle or larger. In the case of KR9912-PC4, the variations in ARM and color reflectance (L*) do not coincide with each other in some parts, which made the correlation more difficult. Even in this core, however, the assigned ages would be better than based only on the magnetostratigraphy.

[23] On the basis of our age model, the Cobb Mountain Subchron occurred at MIS 36 (Figures 9 and 10) and the Reunion Subchron at MISs 81 to 82 (Figures 9 through 12), which agrees with previous results [*Channell et al.*, 2002; *Horng et al.*, 2002].

[24] It is notable in Figures 8 through 13 that tie lines of polarity boundaries are often slightly oblique to those connecting the $\delta^{18}O$ and magnetic concentration curves. The ages of polarity boundaries shown in the panels of the $\delta^{18}O$ curve are after *Cande and Kent* [1995]. Depths of the polarity boundaries observed in the cores tend to be deeper than those expected from the correlation between the $\delta^{18}O$ and magnetic concentration curves. The top of the Olduvai Subchron in MD982185 and the M/G boundary in MD982187 are such examples. This difference is on the order of 10 cm. This may have resulted from the lock-in depth of post-depositional remanent magnetization (pDRM), and/or time lag between $\delta^{18}O$ and the magnetic proxies, *k* and ARM.

## 5. Relative Paleointensity

[25] The six sediment cores have magnetic properties suitable for relative paleointensity estimation, as presented above. Downcore variations in magnetic concentration are within several times. Changes in magnetic grain size and mineralogy are estimated to be small. Relative variations of normalized intensity do not depend on the choice of the normalizer; normalization by ARM and IRM showed almost the same variation patterns (Figures 3 through 7). Even NRM intensities before the normalization do not differ very much from those after the normalization. These results fulfill the criteria for obtaining reliable relative paleointensity [*Tauxe*, 1993].

[26] A remarkable feature is that the cores from the Manihiki Plateau show upward decreasing trends in normalized intensity (Figure 15). These trends are parallel to long-term decreases in sedimentation rate. This implies that sedimentation rate can control normalized intensity even when magnetic concentration, magnetic grain size, and mineralogy are uniform, although the mechanism is unknown. We corrected the effect of sedimentation rate by fitting a linear trend to the normalized intensities and regarding this as the mean (unit) relative paleointensity. For the cores from the West Caroline Basin, on the other hand, no trend was observed in sedimentation rate and normalized intensity before the B/M boundary.

[27] The six relative paleointensity records after converting depths to ages agree well with each

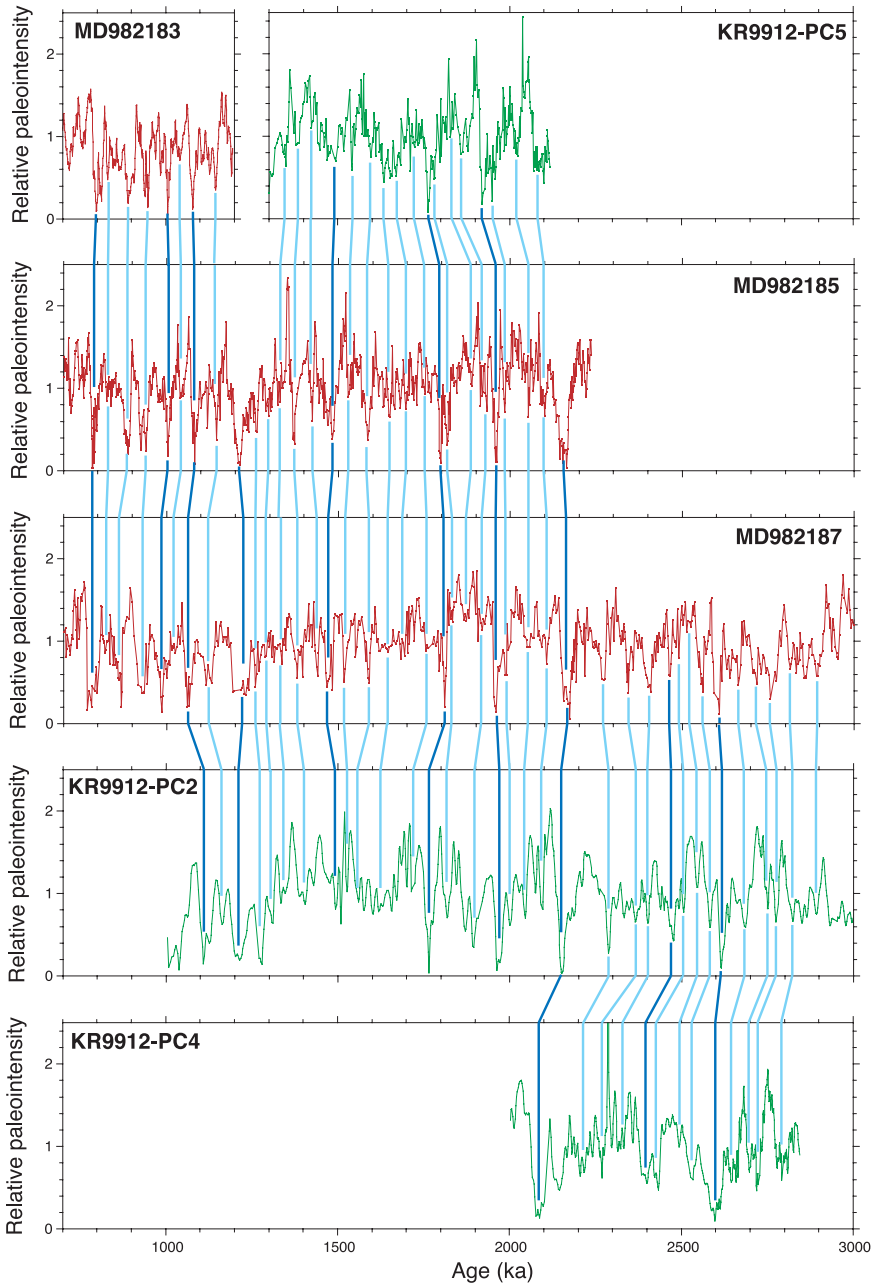


**Figure 16.** Relative paleointensity records of three cores from the West Caroline Basin (red) and three cores from the Manihiki Plateau (green). Succession of peaks and troughs coincides well with each other within uncertainty of age as indicated by correlation lines: dark blue lines for conspicuous lows and pale blue lines for minor lows between them.

other (Figure 16). Even successions of minor peaks and troughs on the order of 10 kyr between major intensity lows are correlative, as shown by tie lines in the figure. Inconsistency in age among the records is about 20 kyr for the cores from the West Caroline Basin, and about one obliquity cycle, 40 to 50 kyr, for the cores from the Manihiki Plateau. Inter-core consistency between the two areas of about 8000 km apart as well as between nearby cores indicates that the normalized intensity records reflect variations in the strength of the geomagnetic dipole field.

[28] We constructed a master curve of relative paleointensity from the B/M boundary to 3 Ma in the equatorial Pacific (equatorial Pacific paleointensity stack, EPAPIS-3Ma) by combining the six records (Figure 17). From 780 to 2160 ka (the

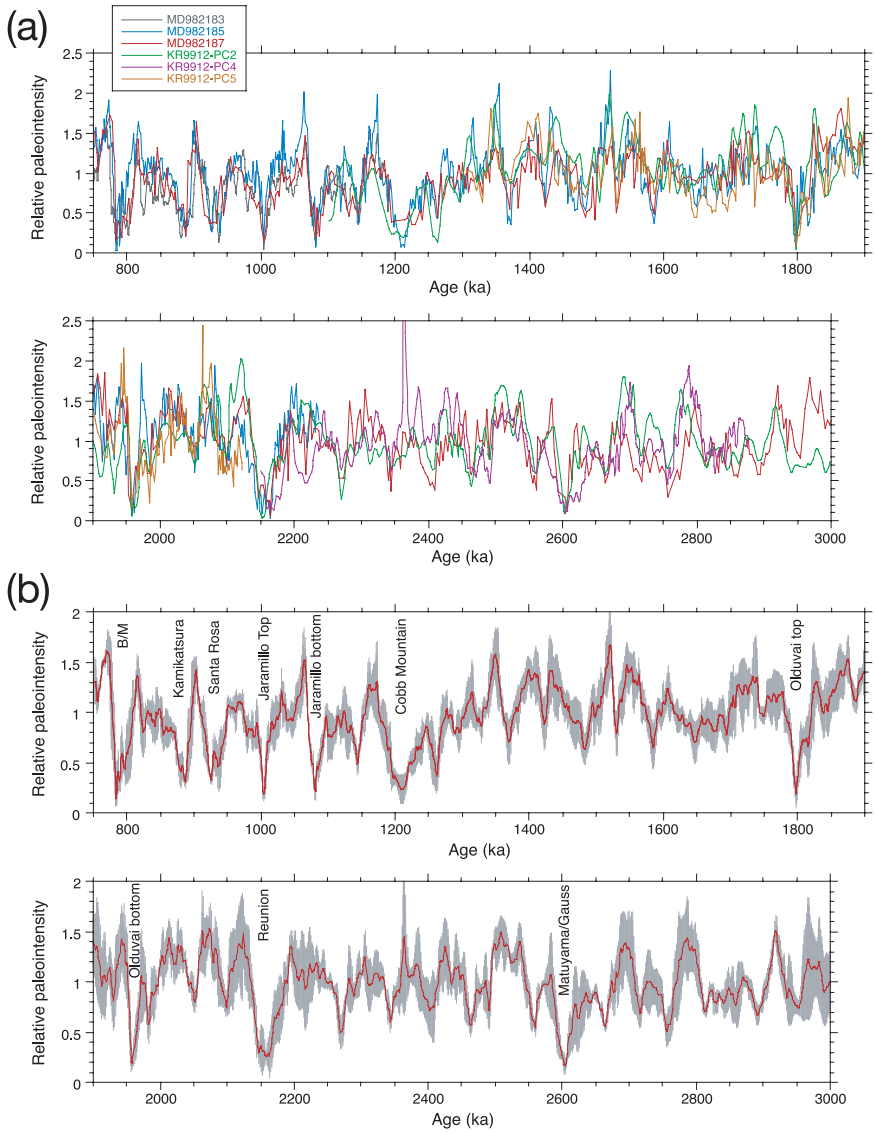


**Figure 17.** (a) All six relative paleointensity records are superimposed after adjusting ages according to the tie lines in Figure 16. (b) Equatorial Pacific paleointensity stack EPAPIS-3Ma. The mean (red) and standard deviation (gray) in a sliding 2 kyr window were calculated after each record was interpolated at 1 kyr intervals.

Reunion Subchron), MD982185 was selected as a reference, and ages of other cores were adjusted at the tie points shown in Figure 16. For the period older than 2160 ka, MD982187 was used as a reference. Next, each record was resampled at 1 kyr intervals by linear interpolation, and all records were superimposed (Figure 17a). Then the mean and standard deviation in a 2 kyr sliding window were calculated (Figure 17b). The number of cores stacked was four between 1200 and 2100 ka, and three for the periods younger and older than this interval.

[29] Correlation between the $\delta^{18}O$ curves and ARM (or color reflectance L* for core KR9912-PC4) after adjusting ages on the basis of the paleointensity correlation is shown in Figure 18. The adjusted age model did not bring significant conflicts among them.

## 6. Discussion

### 6.1. Comparison With Other Records

[30] We compare our relative paleointensity record, the EPAPIS-3Ma, with those of previously published (Figure 19), and discuss common features, which is considered to reflect geomagnetic field variations, and differences. The records of

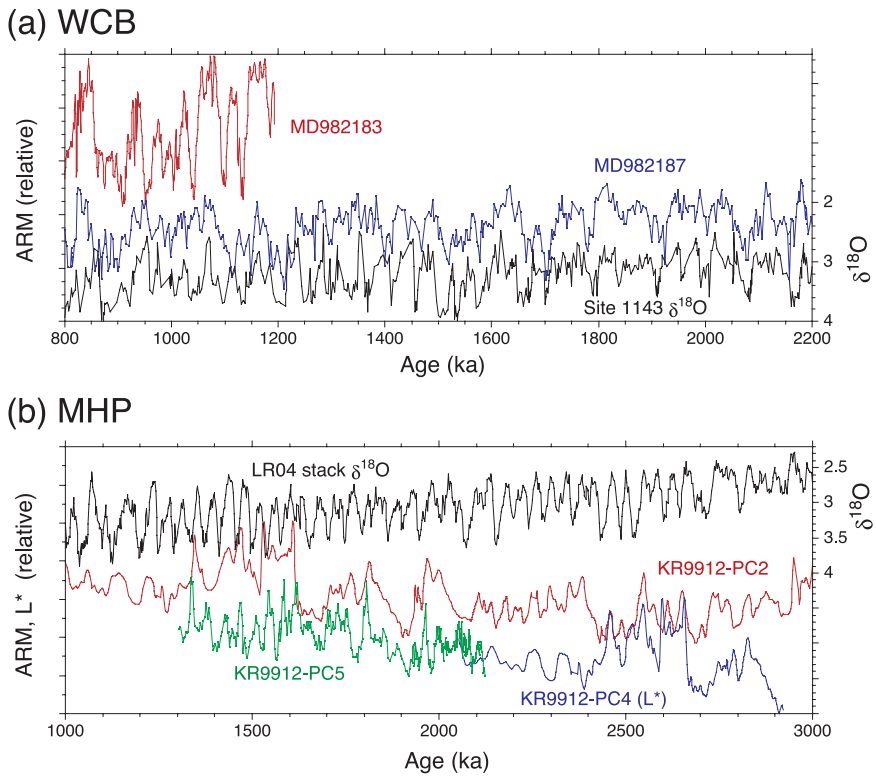


**Figure 18.** Correlation of the $\delta^{18}O$ curves and ARM after adjusting ages based on paleointensity correlation shown in Figure 16. (a) West Caroline Basin. Records of MD982185 and MD982187 of older than 2200 ka are not shown: they are the references with no age adjustment. (b) Manihiki Plateau. Color reflectance L* is shown for KR9912-PC4 instead of ARM.

MD972140 [*Carcaillet et al.*, 2003], MD972143 [*Horng et al.*, 2003], and the OJP-stack [*Kok and Tauxe*, 1999] were obtained from low latitudes of the western Pacific (Figure 1): the Euripik Rise bounding the West and East Caroline Basins (MD972140), the western Philippine Sea off Luzon Island (MD972143), and the Ontong-Java Plateau (the OJP-stack). The record of ODP Leg 138 [*Valet and Meynadier*, 1993] came from the eastern equatorial Pacific, and the record of ODP Site 984 [*Channell et al.*, 2002] was from the North Atlantic.

[31] The variation patterns of MD972140 [*Carcaillet et al.*, 2003], MD972143 [*Horng et al.*, 2003], and the EPAPIS-3Ma agree well in general, and even short-wavelength features on the order of 10 kyr are correlative. However, there are some differences in age among the records, which is about 50 ka at the maximum. The age control of both MD972140 and MD972143 is based on the $\delta^{18}O$ stratigraphy. The discrepancy in age is probably caused by partial miss-assignment of MISs for one obliquity cycle in the three records. A relative paleointensity peak at about 900 ka is missing in the record of MD972143, although it appears in other records. A short hiatus may have occurred in MD972143. Reduced paleointensities below the Olduvai Subchron are observed only in MD972143, which could be caused by magnetic property changes. On the other hand, MD972140 only shows a period of strong paleointensities around 1250 ka, whereas others indicate a decreasing trend from 1350 to 1200 ka.

[32] The record of ODP Site 984 [*Channell et al.*, 2002] shows variations with larger amplitude and shorter wavelength than others. Minimum paleointensity values as small as those associated with polarity boundaries occur frequently during a single polarity in the Site 984 record, whereas corresponding paleointensity lows in other records are not so small. The sedimentation rate at this site is very large, about 115 m/m.y. in average, which is at least several times larger than those of other records. The amplitude of the Site 984 record is considered to be closer to the true geomagnetic field behavior than other records because this record less suffered a low-pass filtering effect caused by pDRM acquisition process and stacking.

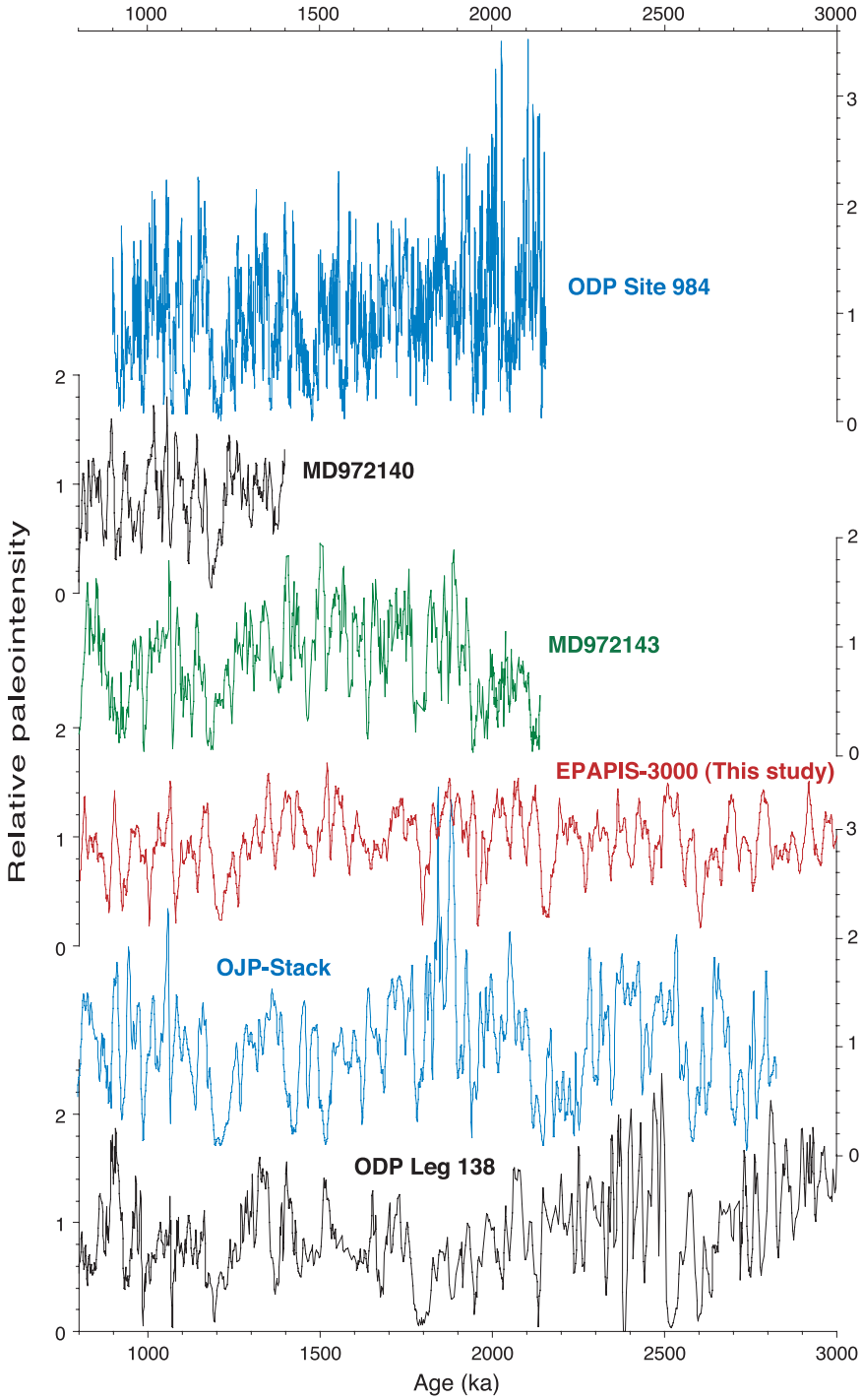


**Figure 19.** Comparison of the equatorial Pacific paleointensity stack EPAPIS-3Ma of this study with previously published records: ODP Site 984 [*Channell et al.*, 2002], MD972140 [*Carcaillet et al.*, 2003], MD972143 [*Horng et al.*, 2003], the OJP stack [*Kok and Tauxe*, 1999], and ODP Leg 138 [*Valet and Meynadier*, 1993].

If we ignore high-frequency components, the general pattern of the variations of the Site 984 record resembles the EPAPIS-3Ma as well as others from the equatorial Pacific. An exception is that the Site 984 record only shows stronger paleointensities before the Olduvai Subchron. Such feature is not recognized in other record and hence may not be true. The ages of the Site 984 record and the EPAPIS-3Ma agree very well with each other. The difference in the ages of the paleointensity

peaks and troughs is 20 kyr or less in general. The age control of the Site 984 record was carried out by the same method as ours; magnetic susceptibility variations were correlated with the reference $\delta^{18}O$ record from ODP Site 677 except for the interval of 0.9 to 1.2 Ma being based on $\delta^{18}O$ data. The close agreement in age between the two records suggests the usefulness of magnetic susceptibility for age estimation.

[33] The succession of paleointensity highs and lows of the OJP-stack [*Kok and Tauxe*, 1999] matches with the EPAPIS-3Ma back to the bottom of the Olduvai Subchron, if the ages of the OJP-stack between 1300 and 1700 ka are shifted toward younger ages by 60 ka at the maximum. For example, a low at about 1430 ka of the OJP-stack can be correlated with a low at about 1370 ka of the EPAPIS-3Ma. The age control of the OJP-stack is based only on the magnetostratigraphy, and thus age uncertainty would be larger than other records. In the OJP-stack, anomalously high paleointensities occur in the Olduvai Subchron, but such peaks are not observed in other records. In the period of older than the Olduvai Subchron, the appearance of the two records differs to some extent, in particular low paleointensities around 2200 ka in the OJP-stack versus highs in the EPAPIS-3Ma. However, paleointensity minima in the two records are still correlative with each other, if slight shifts in ages are allowed; for example the lows at 2150, 2340, 2460, 2560, 2600 (the M/G boundary), 2665, 2715, and 2750 ka in the EPAPIS-3Ma have corresponding lows in the OJP-stack.

[34] The ODP Leg 138 record [*Valet and Meynadier*, 1993] also shows good agreement with the EPAPIS-3Ma between the Jaramillo and Olduvai Subchrons. The age of the ODP Leg 138 record is controlled by orbital tuning of sediment density data, and the age of 2520 ka was adopted for the G/M boundary instead of 2580 or 2600 ka of other records. In the period older than the top of the Olduvai Subchron, however, the agreement between the ODP Leg 138 record and the EPAPIS-3Ma is rather poor. The ODP Leg 138 record shows the "asymmetric sawtooth pattern," but such a trend is not recognized in the EPAPIS-3Ma as well as in the OJP-stack.

[35] Overall, frequent quasiperiodic paleointensity lows are commonly observed in the EPAPIS-3Ma and other paleointensity records during the Matuyama and late Gauss Chrons. Parts of them appear to correspond to previously reported excursions such as the Kamikatsura excursion at about 886 ka and the Santa Rosa excursion at about 922 ka [*Singer et al.*, 1999]. Other paleointensity lows may also accompany excursions [*Channell et al.*, 2002]. This is the same situation as the paleointensity lows in the Brunhes Chron [*Valet and Meynadier*, 1993]. Recent compilation revealed that probably more than 16, possibly up to 23, excursions may exist in the Brunhes Chron, and many of them are associated with relative paleointensity lows [*Oda et al.*, 2004; H. Oda et al., manuscript in preparation, 2005]. This suggests that geomagnetic excursions are caused by relatively larger contribution of non-dipole components when the intensity of the dipole field is low. The quasiperiodic intensity lows accompanied by excursions is not restricted in the Brunhes Chron, and considered to be an intrinsic feature of the geomagnetic field.

[36] The comparison of available paleointensity records during the last 3000 kyr mentioned above have indicated that successions of peaks and troughs agree with each other in general within uncertainty of the ages. However, the amplitudes of the peaks and troughs often disagree. For example, a peak at 1350 ka is less prominent than a peak at 1520 ka in the EPAPIS-3Ma, but it is opposite to the corresponding peaks in the OJP-stack. Non-dipole components of the geomagnetic field cannot be responsible for it, because inconsistency of this kind also occurs among the records from nearby cores: among our three individual records from the West Caroline Basin, and among the three from the Manihiki Plateau. We estimate that variations in sedimentation rate would be the main cause of the difference. Our study revealed that sedimentation rate can significantly influence the normalized intensity, and we corrected for a long-term trend in sedimentation rate changes. Sedimentation rate, however, can fluctuate locally and frequently in time on the order of glacial-interglacial cycles, and such changes are difficult to be quantified and corrected for. In addition, sediment lithology such as clay mineral composition can also affect more or less the normalized intensity [*Franke et al.*, 2004].

## 6.2. Possible Orbital Modulation

[37] A spectral analysis was performed on the paleointensity records of MD982187 between 0.8 and 3.0 Ma and KR9912-PC2 between 1.1 and 3.0 Ma (Figure 20). We selected the two records because they cover longer periods of time than others. We tested two age models, the final age model and the one before being adjusted by

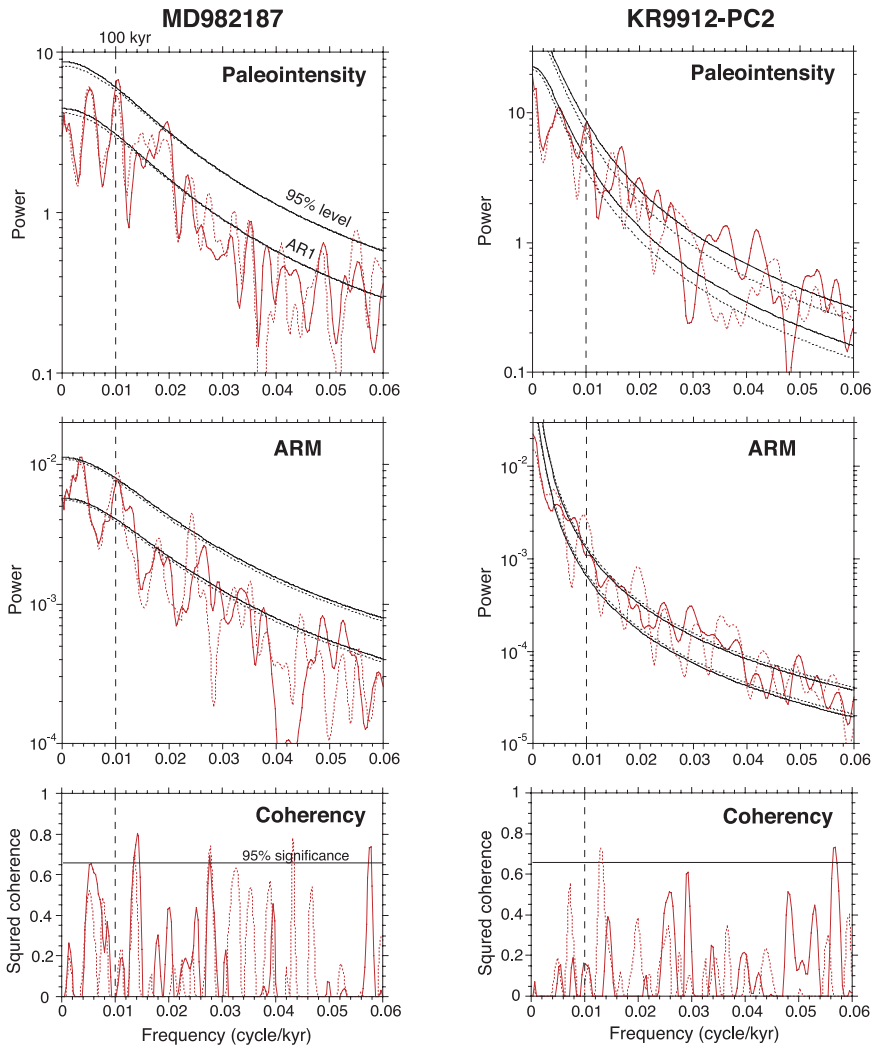


**Figure 20.** Power spectra of relative paleointensity and normalizer (ARM), and cross correlation between them: (left) MD982187 between 0.8 and 3.0 Ma and (right) KR9912-PC2 between 1.1 and 3.0 Ma. Results of two age models are shown: the final age model (solid curves) and the age model before adjustment by paleointensity correlation (dotted curves). The statistical significance of the spectral peaks was tested against the red-noise background from a first-order autoregressive (AR1) process, and the 95% confidence level is indicated. SPECTRUM and REDFIT software [*Schulz and Stattegger*, 1997; *Schulz and Mudelsee*, 2002] for spectral analyses of unevenly spaced time series was used. Welch-Overlapped-Segment-Averaging method was used, and number of segments is four. Hanning window was applied.

the paleointensity correlation. Both paleointensity records show peaks at a period of about 100 kyr in the power spectrum, which coincides with the orbital eccentricity frequency. The occurrence of peaks at ~100 kyr is independent to the age models. The peaks are significant at the 95% confidence level, except for the case of MD982187 with the age model before adjustment, which is close to but not reached to the 95% level. Previously, orbital modulation of the geomagnetic field was proposed mainly on the basis of paleointensity records during the Brunhes Chron [*Channell et al.*, 1998; *Yamazaki*, 1999; *Yokoyama and Yamazaki*, 2000]. This study suggests that the occurrence of the ~100 kyr period is not restricted in the Brunhes Chron, but it would go back to 3 Ma. The existence of the ~100 kyr period in the two cores with little changes in magnetic grain size and mineralogy but of different lithology suggests that the frequency would not have been induced by variations in magnetic properties.

[38] Coherency between relative paleointensity and its normalizer is often used for evaluating lithological contamination of the paleointensity records [e.g., *Tauxe and Wu*, 1990; *Channell et*

*al.*, 1998]. In the records of MD982187 and KR9912-PC2, the normalizer (ARM) also has a significant power at the ~100 kyr period, but coherency between the two is not significant (Figure 20). This result supports that the ~100 kyr period in the paleointensity records would not be caused by sedimentological effects.

[39] If the orbital parameters affect both the geomagnetic field and depositional environment, paleointensity and a normalizer could have significant coherency. Thus we consider that the possibility of orbital modulation of the geomagnetic field cannot be rejected for the reason of coherency with a normalizer. No sediments can be completely homogeneous without any lithological change, and they are more or less affected by paleoenvironmental changes that contain the orbital periodicities. In this respect, coherence analysis may not be a powerful tool for examining sedimentological contamination.

[40] It is still necessary to accumulate further high-quality paleointensity records to establish (or dismiss) the hypothesis of orbital modulation. Relative paleointensity records still contain significant errors, which is indicated by the inconsistency in the amplitude of individual highs and lows. The records also have uncertainty in ages, but within our knowledge, any method of time series analysis assumes no error in time. These factors deteriorate the reliability of the results of spectral analyses. Rock-magnetic studies for evaluating quantitatively the effect of magnetic property changes to relative paleointensity estimation are also required to assess lithological contamination to the orbital frequencies.

## Acknowledgments

[41] We thank Etsuko Usuda for the help of the measurements, Shungo Kawagata for discussion on the ages, Yuhji Yamamoto for comments on the manuscript, and those who concerned the R/V *Kairei* KR99-12 and R/V *Marion Dufresne* IMAGES IV cruises for taking the cores. We also thank constructive comments from the associate editor, Catherine Johnson, and the reviewers, Jim Channell and Joe Stoner, which were useful for improving the paper. This study was partly supported by the Grant-in-Aid for Scientific Research ((C)(2) 14540402 and (A)(2) 16204034) of the Japan Society for the Promotion of Science, and the "Superplume Project" of the Ministry of Education, Culture, Sports, Science and Technology.

## References

Archer, D., A. Winguth, D. Lea, and N. Mahowald (2000), What caused the glacial/interglacial atmospheric $pCO_2$ cycles?, *Rev. Geophys.*, *38*, 159–189.

Berger, W. H., C. G. Adelseck Jr., and L. A. Mayer (1976), Distribution of carbonate in surface sediments of the Pacific Ocean, *J. Geophys. Res.*, *81*, 2617–2627.

Bloemendal, J., J. W. King, F. R. Hall, and S.-J. Doh (1992), Rock magnetism of Late Neogene and Pleistocene deep-sea sediments: Relationship to sediment source, diagenetic processes, and sediment lithology, *J. Geophys. Res.*, *97*, 4361–4375.

Cande, S. C., and D. V. Kent (1995), Revised calibration of the geomagnetic polarity timescale for the Late Cretaceous and Cenozoic, *J. Geophys. Res.*, *100*, 6093–6095.

Carcaillet, J. T., N. Thouveny, and D. L. Bourlès (2003), Geomagnetic moment instability between 0.6 and 1.3 Ma from cosmonuclide evidence, *Geophys. Res. Lett.*, *30*(15), 1792, doi:10.1029/2003GL017550.

Channell, J. E. T., D. A. Hodell, J. McManus, and B. Lehman (1998), Orbital modulation of the Earth's magnetic field intensity, *Nature*, *394*, 464–468.

Channell, J. E. T., A. Mazaud, P. Sullivan, S. Turner, and M. E. Raymo (2002), Geomagnetic excursions and paleointensities in the Matuyama Chron at Ocean Drilling Program Sites 983 and 984 (Iceland Basin), *J. Geophys. Res.*, *107*(B6), 2114, doi:10.1029/2001JB000491.

Channell, J. E. T., J. Labs, and M. E. Raymo (2003), The Reunion subchronozone at ODP Site 981 (Feni Drift, North Atlantic), *Earth Planet. Sci. Lett.*, *215*, 1–12.

Franke, C., D. Hofmann, and T. von Dobeneck (2004), Does lithology influence relative paleointensity records? A statistical analysis on South Atlantic pelagic sediments, *Phys. Earth Planet. Inter.*, *147*, 285–296.

Guyodo, Y., and J.-P. Valet (1999), Global changes in intensity of the Earth's magnetic field during the past 800 kyr, *Nature*, *399*, 249–252.

Guyodo, Y., P. Gaillot, and J. E. T. Channell (2000), Wavelet analysis of relative geomagnetic paleointensity at ODP Site 983, *Earth Planet. Sci. Lett.*, *184*, 109–123.

Horng, C.-S., M.-Y. Lee, H. Palike, K.-Y. Wei, W.-T. Liang, Y. Iizuka, and M. Torii (2002), Astronomically calibrated ages for geomagnetic reversals within the Matuyama chron, *Earth Planets Space*, *54*, 679–690.

Horng, C., A. P. Roberts, and W. Liang (2003), A 2.14-Myr astronomically tuned record of relative geomagnetic paleointensity from the western Philippine Sea, *J. Geophys. Res.*, *108*(B1), 2059, doi:10.1029/2001JB001698.

Kirschvink, J. L. (1980), The least-squares line and plane and the analysis of paleomagnetic data, *Geophys. J. R. Astron. Soc.*, *62*, 699–718.

Kok, Y. S. (1999), Climatic influence in NRM and $^{10}$Be-derived geomagnetic paleointensity data, *Earth Planet. Sci. Lett.*, *166*, 105–119.

Kok, Y. S., and L. Tauxe (1996), Saw-toothed pattern of relative paleointensity records and cumulative viscous remanence, *Earth Planet. Sci. Lett.*, *137*, 95–99.

Kok, Y. S., and L. Tauxe (1999), A relative geomagnetic paleointensity stack from Ontong-Java Plateau sediments for the Matuyama, *J. Geophys. Res.*, *104*, 25,401–25,413.

Laj, C., C. Kissel, A. Mazaud, J. E. T. Channell, and J. Beer (2000), North Atlantic palaeointensity stack since 75 ka (NAPIS-75) and the duration of the Laschamp event, *Philos. Trans. R. Soc. London, Ser. A*, *358*, 1009–1024.

Lisiecki, L. E., and M. E. Raymo (2005), A Pliocene-Pleistocene stack of 57 globally distributed benthic $\delta^{18}$O records, *Paleoceanography*, *20*, PA1003, doi:10.1029/2004PA001071.

Mazaud, A. (1996), 'Sawtooth' variation in magnetic intensity profiles and delayed acquisition of magnetization in deep sea cores, *Earth Planet. Sci. Lett.*, *139*, 379–386.

Meynadier, L., J.-P. Valet, F. C. Bassinot, N. J. Shackleton, and Y. Guyodo (1994), Asymmetric saw-tooth pattern of the geomagnetic field intensity from equatorial sediments in the Pacific and the Indian Oceans, *Earth Planet. Sci. Lett.*, *126*, 109–127.

Oda, H., and H. Shibuya (1994), Deconvolution of whole-core magnetic remanence data by ABIC minimization, *J. Geomagn. Geoelectr.*, *46*, 613–628.

Oda, H., and H. Shibuya (1996), Deconvolution of long-core paleomagnetic data of Ocean Drilling Program by Akaike's Bayesian Information Criterion minimization, *J. Geophys. Res.*, *101*, 2815–2834.

Oda, H., M. J. Dekkers, C. G. Lagereis, L. Lourens, and D. Heskop (2004), A paleomagnetic record of the last 640 kyr from an eastern Mediterranean piston core and a review of geomagnetic excursions in the Brunhes, *Eos Trans. AGU*, *85*(47), Fall Meet. Suppl., Abstract GP41B-08.

Schulz, M., and M. Mudelsee (2002), REDFIT: Estimating red-noise spectra directly from unevenly spaced paleoclimatic time series, *Comput. Geosci.*, *28*, 421–426.

Schulz, M., and K. Stattegger (1997), SPECTRUM: Spectral analysis of unevenly spaced paleoclimatic time series, *Comput. Geosci.*, *23*, 929–945.

Singer, B. S., K. A. Hoffman, A. Chauvin, R. S. Coe, and M. S. Pringle (1999), Dating transitionally magnetized lavas of the late Matuyama Chron: Toward a new $^{40}Ar/^{39}Ar$ timescale of reversals and events, *J. Geophys. Res.*, *104*, 679–693.

Stoner, J. S., J. E. T. Channell, C. Hillaire-Marcel, and C. Kissel (2000), Geomagnetic paleointensity and environmental record from Labrador Sea core MD95–2024: Global marine sediment and ice core chronostratigraphy for the last 110 kyr, *Earth Planet. Sci. Lett.*, *183*, 161–177.

Sugiura, N. (1979), ARM, TRM and magnetic interactions: Concentration dependence, *Earth Planet. Sci. Lett.*, *42*, 451–455.

Tauxe, L. (1993), Sedimentary records of relative paleointensity of the geomagnetic field: Theory and practice, *Rev. Geophys.*, *31*, 319–354.

Tauxe, L., and G. Wu (1990), Normalized remanence in sediments of the western equatorial Pacific: Relative paleointensity of the geomagnetic field?, *J. Geophys. Res.*, *95*, 12,337–12,350.

Tian, J., P. Wang, X. Cheng, and Q. Li (2002), Astronomically tuned Plio-Pleistocene benthic $\delta^{18}O$ record from South China Sea and Atlantic-Pacific comparison, *Earth Planet. Sci. Lett.*, *203*, 1015–1029.

Valet, J.-P., and L. Meynadier (1993), Geomagnetic field intensity and reversals during the past four million years, *Nature*, *366*, 234–238.

Yamada, S., K. Akimoto, S. Kawagata, T. Yamazaki, and H. Oda (2000), The distribution of sediments on and around the Manihiki Plateaus, Central Pacific Ocean—Sedimentological description of the seven core samples obtained by R/V Kairei KR99–12 cruise, *JAMSTEC J. Deep Sea Res.*, *17*, 95–156.

Yamazaki, T. (1999), Relative paleointensity of the geomagnetic field during Brunhes Chron recorded in North Pacific deep-sea sediment cores: Orbital influence?, *Earth Planet. Sci. Lett.*, *169*, 23–35.

Yamazaki, T., and N. Ioka (1994), Long-term secular variation of the geomagnetic field during the last 200 kyr recorded in sediment cores from the western equatorial Pacific, *Earth Planet. Sci. Lett.*, *128*, 527–544.

Yamazaki, T., and N. Ioka (1997), Cautionary note on magnetic grain-size estimation using the ratio of ARM to magnetic susceptibility, *Geophys. Res. Lett.*, *24*, 751–754.

Yamazaki, T., and H. Oda (2002), Orbital influence on Earth's magnetic field: 100,000-year periodicity in inclination, *Science*, *295*, 2435–2438.

Yamazaki, T., and H. Oda (2004), Intensity-inclination correlation on long-term secular variation of the geomagnetic field and its relevance to persistent non-dipole component, in *Timescales of the Internal Geomagnetic Field*, *Geophys. Monogr. Ser.*, vol. 145, edited by J. E. T. Channell et al., pp. 287–298, AGU, Washington, D. C.

Yamazaki, T., A. L. Abdeldayem, and K. Ikehara (2003), Rock-magnetic changes with reduction diagenesis in Japan Sea sediments and preservation of geomagnetic secular variation in inclination during the last 30,000 years, *Earth Planets Space*, *55*, 327–340.

Yokoyama, Y., and T. Yamazaki (2000), Geomagnetic paleointensity variation with a 100 kyr quasi-period, *Earth Planet. Sci. Lett.*, *181*, 7–14.